

Fluctuoscopia of Disordered Two-Dimensional Superconductors

A. Glatz,¹ A. A. Varlamov,^{1,2} and V. M. Vinokur¹

¹Materials Science Division, Argonne National Laboratory,
9700 S.Cass Avenue, Argonne, Illinois 60637, USA

²CNR-SPIN, Viale del Politecnico 1, I-00133 Rome, Italy

(Dated: November 3, 2018)

We revise the long studied problem of fluctuation conductivity (FC) in disordered two-dimensional superconductors placed in a perpendicular magnetic field by finally deriving the complete solution in the temperature-magnetic field phase diagram. The obtained expressions allow both to perform straightforward (numerical) calculation of the FC surface $\delta\sigma_{xx}^{(\text{tot})}(T, H)$ and to get asymptotic expressions in all its qualitatively different domains. This surface becomes in particular non-trivial at low temperatures, where it is trough-shaped with $\delta\sigma_{xx}^{(\text{tot})}(T, H) < 0$. In this region, close to the quantum phase transition, $\delta\sigma_{xx}^{(\text{tot})}(T, H = \text{const})$ is non-monotonic, in agreement with experimental findings. We reanalyzed and present comparisons to several experimental measurements. Based on our results we derive a qualitative picture of superconducting fluctuations close to $H_{c2}(0)$ and $T = 0$ where fluctuation Cooper pairs rotate with cyclotron frequency $\omega_c \sim \Delta_{\text{BCS}}^{-1}$ and Larmor radius $\sim \xi_{\text{BCS}}$, forming some kind of quantum liquid with long coherence length $\xi_{\text{QF}} \gg \xi_{\text{BCS}}$ and slow relaxation ($\tau_{\text{QF}} \gg \hbar\Delta_{\text{BCS}}^{-1}$).

I. INTRODUCTION

The understanding of the mechanisms of superconducting fluctuations (SF), achieved during the past decades¹ provided a unique tool obtaining information about the microscopic parameters of superconductors (SC). SFs are comprised of Cooper pairs with finite lifetime which appear already above the transition but do not form a stable condensate yet. They affect thermodynamic and transport properties of the normal state both directly and through the changes which they cause in the normal quasi-particle subsystem¹.

SFs are commonly described in terms of three principal contributions: the Aslamazov-Larkin (AL) process, corresponding to the opening of a new channel for the charge transfer², anomalous Maki-Thompson (MT) process, which describes single-particle quantum interference at impurities in the presence of SFs^{3,4}, and the change of the single-particle density of states (DOS) due to their involvement in fluctuation pairings^{5,6}. The first two processes (AL and MT) result in the appearance of positive and singular contributions to conductivity (diagrams 1 and 2 in Fig. 1) close to the superconducting critical temperature T_{c0} , while the third one (DOS) results in a decrease of the Drude conductivity due to the lack of single-particle excitations at the Fermi level (diagrams 3-6 in Fig. 1). The latter contribution is less singular in temperature than the first two and can compete with them only if the AL and MT processes are suppressed for some reasons (for example, c-axis transport in layered superconductors) or far away from T_{c0} .

The classical results obtained first in the vicinity of T_{c0} were later generalized to temperatures far from the transition, e.g. in Refs. [7–9], and to relatively high fields, see Ref. [10]. More recently, quantum fluctuations (QF) came into the focus of investigations. In Ref. [11 and 12] it was found, that in granular SC at very low tempera-

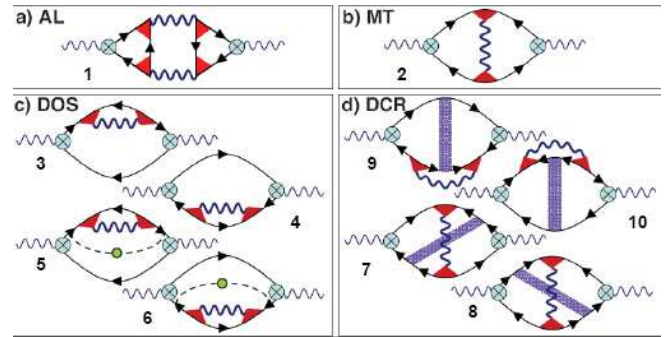


FIG. 1. (Color online) Feynman diagrams for the leading-order contributions to the electromagnetic response operator. Wavy lines stand for fluctuation propagators, solid lines with arrows are impurity-averaged normal state Green's functions, crossed circles are electric field vertices, dashed lines with a circle represent additional impurity renormalizations, and triangles and dotted rectangles are impurity ladders accounting for the electron scattering at impurities (Cooperons).

tures and close to $H_{c2}(0)$, the positive AL contribution to magneto-conductivity decays as T^2 while the fluctuation suppression of the DOS results in a temperature independent negative contribution, logarithmically growing in magnitude for $H \rightarrow H_{c2}(0)$. The authors of Ref. [13] came to the same conclusion while studying the effect of QFs on the Nernst-Ettingshausen coefficient in two-dimensional (2D) SCs. For the first time they attracted the attention¹⁴ to the special role of diagrams 9 & 10 in Fig. 1.

Special attention should be paid to the paper by Galitski and Larkin, Ref. [15], where the effects of QFs on magneto-conductivity and magnetization of 2D superconductors were studied. The authors analyzed all ten diagrams shown in Fig. 1 in the lowest Landau level

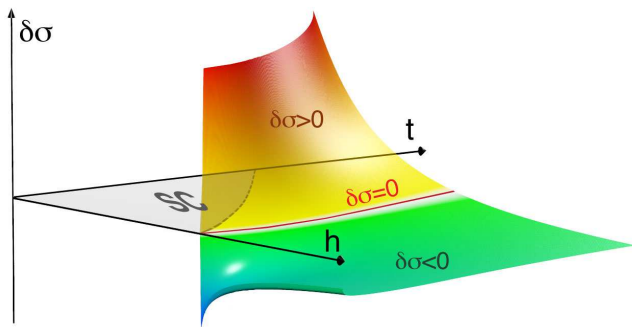


FIG. 2. (Color online) Fluctuation correction to conductivity (FC) $\delta\sigma = \delta\sigma_{xx}^{(\text{tot})}(t, h)$ as function of the reduced temperature $t = T/T_{c0}$ and magnetic field $h = 0.69H/H_{c2}(0)$ plotted as surface. The FC changes its sign along the thick red line ($\delta\sigma = 0$). The boundary of the superconducting region is shown by a dashed line. Here $\delta\sigma$ is plotted for constant $\tau T_{c0} = 10^{-2}$ and $\tau_{\phi} T_{c0} = 10$.

(LLL) approximation, valid at fields close to the critical line $H_{c2}(T)$. They found an expression for the total fluctuation contribution to magneto-conductivity in this region and demonstrated that, analogously to the situation in granular SCs, close to zero temperature and in the vicinity of $H_{c2}(0)$ this contribution is negative, i.e. QFs increase resistivity, and not conductivity (in contrast to the situation close to T_{c0}). Nevertheless, contrary to the conclusions of Refs. [11 and 12], in Ref. [15] the logarithmic growth of the magneto-resistance at zero temperature when the magnetic field approaches $H_{c2}(0)$ from larger fields, is due to *all* AL, MT and DOS-like contributions.

Yet, the confidence in the exotic nature of negative fluctuation corrections and the common believe of fluctuation contributions to conductivity being positive beyond the narrow domain of the quantum phase transition, has been persistent and is based on available asymptotic expressions only. The region near $T = 0$ and magnetic fields near $H_{c2}(0)$ remains poorly understood and in addition, an universal picture combining QFs at high magnetic fields and conventional finite temperature quantum corrections is still lacking.

This is why we revisit the problem of fluctuation conductivity of a disordered 2D superconductor placed in a perpendicular magnetic field in this paper. We present an exact calculation (*without the use of the LLL approximation*) of all ten diagrams of the first order of fluctuation theory (see Fig. 1) valid in the whole H - T phase diagram beyond the superconducting region, i.e. for arbitrary fields $H \geq H_{c2}(T)$ and temperatures $T_c(H) \leq T$. The obtained expressions allow both to perform straightforward (numerical) calculation of the fluctuation conductivity "surface" $\delta\sigma_{xx}^{(\text{tot})}(T, H)$ and to get asymptotic expressions in all its qualitatively different domains.

A typical example of the surface $\delta\sigma_{xx}^{(\text{tot})}(T, H)$ is pre-

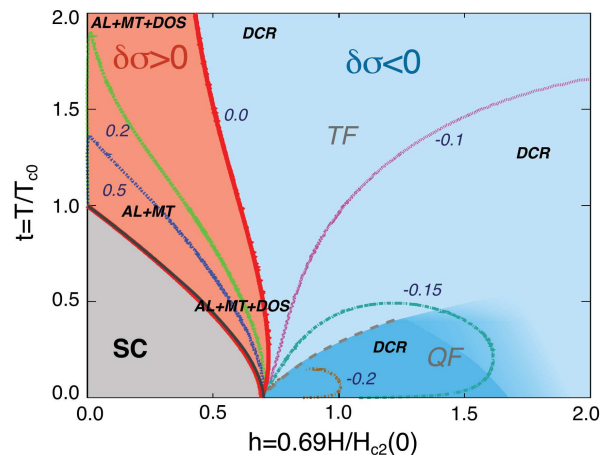


FIG. 3. (Color online) Contours of constant fluctuation conductivity [$\delta\sigma = \delta\sigma_{xx}^{(\text{tot})}(t, h)$ shown in units of e^2]. The dominant FC contributions are indicated by bold-italic labels. The dashed line separates the domain of quantum fluctuations (QF) [dark area of $\delta\sigma < 0$] and thermal fluctuations (TF). The contour lines are obtained from Eq. (3) with $T_{c0}\tau = 0.01$ and $T_{c0}\tau_{\phi} = 10$.

sented in Fig. 2 and demonstrates that our revision and completion of the commonly believed understanding of fluctuation corrections is urgently called for: Its striking feature consists of the fact, that the FC is positive only in the domain bound by the separatrices $H_{c2}(T)$ and $\delta\sigma_{xx}^{(\text{tot})}(T, H) = 0$ and is negative throughout all other parts of the phase diagram (see Fig. 3, in which the domains of different overall signs of $\delta\sigma_{xx}^{(\text{tot})}(T, H)$ and contours of constant $\delta\sigma_{xx}^{(\text{tot})}$ in the whole phase diagram are shown). Contrary to the common assumption, the FC is only positive in the domain of weak fields and temperatures above T_{c0} , the region of positive corrections depends on the magnitude of the positive anomalous MT contribution (i.e. on the value of the phase-breaking time τ_{ϕ}). With increasing magnetic field, the interval of temperatures where $\delta\sigma_{xx}^{(\text{tot})}(T, H) > 0$ shrinks and becomes zero close to $H_{c2}(0)$. In particular at low temperatures, the behavior of the FC turns out to be highly non-trivial. In this case, the surface $\delta\sigma_{xx}^{(\text{tot})}(T, H)$ has a trough-shaped character and the dependence $\delta\sigma_{xx}^{(\text{tot})}(T, H = \text{const})$ is non-monotonic. We will see below that this feature is observed in available experimental results as well.

Our analysis also elucidates the understanding of the hierarchy of the various contributions to the fluctuation corrections in different domains of the phase diagram (see Fig. 3 in which the dominating fluctuation contributions to magneto-conductivity are indicated for different regions of the phase diagram). We reproduce the expression for the total fluctuation contribution to magneto-conductivity of 2D disordered superconductors presented in Ref. [15] in the vicinity of the $H_{c2}(T)$ line. Neverthe-

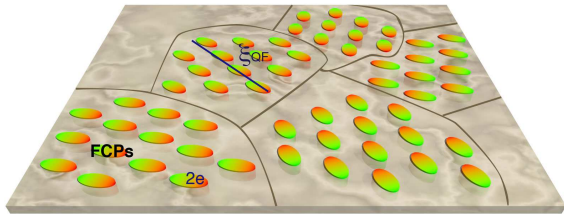


FIG. 4. (Color online) Illustration of the cluster structure of a FCP ($2e$) liquid above the upper critical field. This picture represents a snapshot at a certain time and would stay that way for time τ_{QF} . The typical size of a coherent FCP cluster is ξ_{QF} .

less, our analysis clearly demonstrates that the principal fluctuation contributions close to T_{c0} , paraconductivity (AL), anomalous MT and DOS, in the region of QF become *zero* as $\sim T^2$ (compare to Refs. [11 and 12]) - which is contrary to the picture given in Ref. [15]. It is the fourth, usually ignored, fluctuation contribution, formally determined by the sum of diagrams 7-10 and the regular part of the MT diagram, which governs the quantum phase transition (QPT). It can be identified with the renormalization of the single-particle diffusion coefficient in the presence of fluctuations (DCR) and it turns out that this contribution dominates in the periphery of the phase diagram including the vicinity of the QPT $[t = T/T_{c0} \ll \tilde{h} = (H - H_{c2}(0))/H_{c2}(0); H > H_{c2}(0)]$.

Finally, based on our results, we propose a qualitative picture for QPT, which drastically differs from the Ginzburg-Landau one, valid close to T_{c0} . The latter can be described in terms of a set of long-wavelength fluctuation modes [with $\lambda \gtrsim \xi_{GL}(T) \gg \xi_{BCS}$] of the order parameter, with characteristic lifetime $\tau_{GL} = \pi\hbar/8k_B(T - T_{c0})$. Near the QPT, the order parameter oscillates on much smaller scales - the fluctuation modes with wave-lengths up to ξ_{BCS} are excited. Due to the magnetic field, one can imagine that FCP in this region rotate with the Larmor radius $\sim \xi_{BCS}$ and cyclotron frequency $\omega_c \sim \Delta_{BCS}^{-1}$. We show that close to $H_{c2}(0)$ these FCP form some kind of quantum liquid with long coherence length $\xi_{QF} \sim \xi_{BCS}/\hbar^{1/2}$ and slow relaxation $\tau_{QF} \sim \hbar\Delta_{BCS}^{-1}/\hbar$ (see Fig. 4).

In the following sections and in the appendices, we will show the details of our derivations and calculation and present the general expression for the fluctuation magneto-conductivity of disordered 2D SC throughout the whole phase diagram. For the calculation of the complete and various fluctuation corrections (by numerical integration and summation), we developed an optimized program which is available at [16]. It can be used as the theoretical basis for the “fluctuoscapy” of superconductors: the study of their behavior in ultra-high magnetic fields and precise extraction for their physical parameters like the critical temperature and magnetic field, and

the temperature dependence of the phase-breaking time, and/or e.g. for the separation of the quantum corrections in studies of the “superconductor–insulator” transition.

II. MODEL

We consider a disordered 2D superconductor characterized by the diffusion coefficient \mathcal{D} placed in a perpendicular magnetic field H at temperatures $T > T_c(H)$. Temperatures should not be too close to the critical temperature and remain beyond the region of critical fluctuations, i.e. $T/T_c(H) - 1 \gg \sqrt{Gi_{(2)}}(H)$. The Ginzburg-Levanyuk number $Gi_{(2)}$ for conductivity (see Ref. [1]) in both extremes of the line $H_{c2}(T)$ (at temperatures close to T_{c0} and at zero temperature) is on the order of $(p_F^2 l d)^{-1}$, where d is the SC film thickness, and it can reach values of up to 10^{-2} . We assume the temperature $T \ll \min\{\tau^{-1}, \omega_D\}$ in order to remain in the diffusive regime of electron scattering and in the frameworks of the BCS model (τ is the electron elastic scattering time on impurities, ω_D is the Debye frequency). The restrictions on magnetic field are dictated by the requirements to be below the regime of Shubnikov-de Haas oscillations [$\omega_c \tau \lesssim 1 \iff H \lesssim (T_{c0}\tau)^{-1} H_{c2}(0)$, where $\omega_c = 4\mathcal{D}eH$ is the fluctuation Cooper pair cyclotron frequency] and to be below the Clogston limit: $H \lesssim (\varepsilon_F \tau) H_{c2}(0)$, i.e. $H/H_{c2}(0) \ll \min\{(T_{c0}\tau)^{-1}, \varepsilon_F \tau\}$.

Under these rather non-restrictive assumptions the DC fluctuation conductivity

$$\delta\sigma^{(fl)}(T, H) = - \lim_{\omega \rightarrow 0} \frac{\text{Im}Q^{(fl)}(\omega, T, H)}{\omega} \quad (1)$$

is determined by the imaginary part of the fluctuation contribution $Q^{(fl)}(\omega, T, H)$ to the electromagnetic response operator¹. The latter is described graphically by the ten standard diagrams shown in Fig. 1. The solid lines denote the one-electron Green function

$$G(x, x', p_y, p_z, \varepsilon_l) = \sum_k \frac{\varphi_k(x - l_H^2 p_y) \varphi_k^*(x' - l_H^2 p_y)}{i\varepsilon_l - \xi(k, p_z)},$$

wavy lines correspond to the fluctuation propagator

$$L_n^{-1}(\Omega_k) = -\nu_0 \left[\ln \frac{T}{T_{c0}} + \psi \left(\frac{1}{2} + \frac{|\Omega_k| + \omega_c(n + \frac{1}{2})}{4\pi T} \right) - \psi \left(\frac{1}{2} \right) \right] \quad (2)$$

and shaded three- and four-leg blocks indicate the results of the average over elastic impurity scattering of electrons (Cooperons):

$$\lambda_n(\varepsilon_1, \varepsilon_2) = \frac{\tau^{-1}\theta(-\varepsilon_1\varepsilon_2)}{|\varepsilon_1 - \varepsilon_2| + \omega_c(n + 1/2) + \tau_\varphi^{-1}},$$

$$C_n(\varepsilon_1, \varepsilon_2) = \frac{1}{2\pi\nu_0\tau} \frac{\tau^{-1}\theta(-\varepsilon_1\varepsilon_2)}{|\varepsilon_1 - \varepsilon_2| + \omega_c(n + 1/2) + \tau_\varphi^{-1}}.$$

Here ν_0 is the one-electron density of states, n, m are the quantum numbers of the Cooper pair Landau states, $\Omega_k = 2\pi kT$, $\varepsilon_l = 2\pi T(l + 1/2)$ are the bosonic and fermionic Matsubara frequencies. An important characteristic of these expressions is that they are valid even far from the critical temperature [for temperatures $T \ll \min\{\tau^{-1}, \omega_D\}$] and for $|\Omega_k| \ll \omega_D$ and $n \ll (T_{c0}\tau)^{-1}$.

In the Appendices we present the details of the calculation of all ten diagrams performed under the above general assumptions. In the following sections of the main text, we restrict ourselves to the discussion and analysis

of the main result: the complete expression of the fluctuations corrections and the individual contributions from AL, MT, DOS, and DCR processes.

III. RESULTS

The complete expression for the total fluctuation correction to conductivity $\delta\sigma_{xx}^{(\text{tot})}(T, H)$ of a disordered 2D SC in a perpendicular magnetic field that holds in the complete T - H phase diagram above the line $H_{c2}(T)$ is given by the sum of Eqs. (A15), (B7), (C7), and (D10):

$$\begin{aligned} \delta\sigma_{xx}^{(\text{tot})}(t, h) = & \underbrace{\frac{e^2}{\pi} \sum_{m=0}^{\infty} (m+1) \int_{-\infty}^{\infty} \frac{dx}{\sinh^2 \pi x} \left\{ \frac{\text{Im}^2 \mathcal{E}_m}{|\mathcal{E}_m|^2} + \frac{\text{Im}^2 \mathcal{E}_{m+1}}{|\mathcal{E}_{m+1}|^2} + \frac{\text{Im}^2 \mathcal{E}_{m+1} - \text{Im}^2 \mathcal{E}_m}{|\mathcal{E}_m|^2 |\mathcal{E}_{m+1}|^2} \text{Re}[\mathcal{E}_m \mathcal{E}_{m+1}] \right\}}_{\delta\sigma_{xx}^{\text{AL}}} \\ & + \underbrace{\frac{e^2}{\pi} \left(\frac{h}{t}\right) \sum_{m=0}^M \frac{1}{\gamma_\phi + \frac{2h}{t}(m+1/2)} \int_{-\infty}^{\infty} \frac{dx}{\sinh^2 \pi x} \frac{\text{Im}^2 \mathcal{E}_m}{|\mathcal{E}_m|^2}}_{\delta\sigma_{xx}^{\text{MT(an)}} + \delta\sigma_{xx}^{\text{MT(reg2)}}} + \underbrace{\frac{e^2}{\pi^4} \left(\frac{h}{t}\right) \sum_{m=0}^M \sum_{k=-\infty}^{\infty} \frac{4\mathcal{E}_m''(t, h, |k|)}{\mathcal{E}_m(t, h, |k|)}}_{\delta\sigma_{xx}^{\text{MT(reg1)}}} \\ & + \underbrace{\frac{4e^2}{\pi^3} \left(\frac{h}{t}\right) \sum_{m=0}^M \int_{-\infty}^{\infty} \frac{dx}{\sinh^2 \pi x} \frac{\text{Im} \mathcal{E}_m \text{Im} \mathcal{E}_m'}{|\mathcal{E}_m|^2}}_{\delta\sigma_{xx}^{\text{DOS}}} + \underbrace{\frac{4e^2}{3\pi^6} \left(\frac{h}{t}\right)^2 \sum_{m=0}^M (m + \frac{1}{2}) \sum_{k=-\infty}^{\infty} \frac{8\mathcal{E}_m'''(t, h, |k|)}{\mathcal{E}_m(t, h, |k|)}}_{\delta\sigma_{xx}^{7-10}}. \quad (3) \end{aligned}$$

Here $t = T/T_{c0}$,

$$h = \frac{\pi^2}{8\gamma_E} \frac{H}{H_{c2}(0)} = 0.69 \frac{H}{H_{c2}(0)},$$

$\gamma_E = e^{\gamma_e}$ (γ_e is the Euler constant), $M = (tT_{c0}\tau)^{-1}$, $\gamma_\phi = \pi/(8T_{c0}\tau_\phi)$, τ_ϕ is the phase-breaking time,

$$\mathcal{E}_m \equiv \mathcal{E}_m(t, h, z) = \ln t + \psi \left[\frac{1+z}{2} + \frac{2h(2m+1)}{t\pi^2} \right] - \psi \left(\frac{1}{2} \right)$$

and its derivatives $\mathcal{E}_m^{(p)}(t, h, z) \equiv \partial_z^p \mathcal{E}_m(t, h, z)$. Apart from the detailed derivation of the result, Eq. (3), one can also do a careful study of the asymptotic expressions for different fluctuation contributions throughout the h - t phase diagram, presented in the Appendices. All of them, side by side with the asymptotic expressions for $\delta\sigma_{xx}^{(\text{tot})}$ are summarized in table I.

We start the discussion of table I for domains I -III, corresponding to the Ginzburg-Landau region of fluctuations close to T_{c0} and in zero magnetic field (domain I). One can see, that our general expression Eq. (3) naturally reproduces the well known AL, MT and DOS contributions. The only new result here is the explicitly written contribution $\delta\sigma^{(\text{DCR})}$ (diagrams 7-10), which was usually ignored in view of the lack of its divergence close

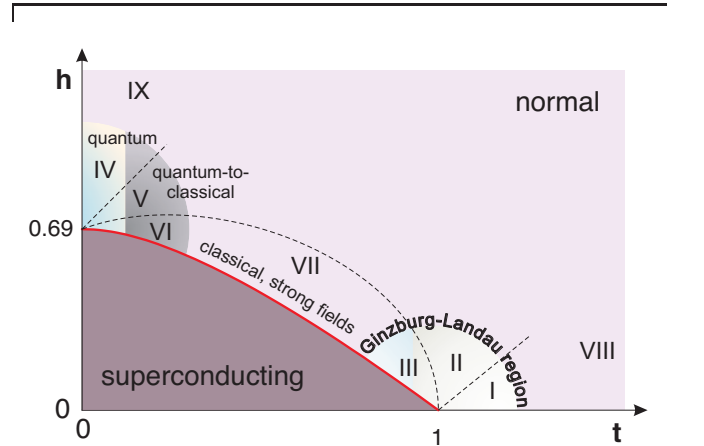


FIG. 5. (Color online) Schematic representation of the regions of different behavior of fluctuation conductivity in the h - t diagram. See table II for more explanations on the domains.

to T_{c0} . Nevertheless, one can see that its constant contribution $\sim \ln \ln (T_{c0}\tau)^{-1}$ is necessary for matching the GL results with the neighboring domains VIII & IX. The domains II & III are still described by the GL theory in weak magnetic fields and Eq. (3) reproduces all available asymptotic expressions found in literature.

	$\delta\sigma_{xx}^{\text{AL}}$	$\delta\sigma_{xx}^{\text{MT}}$	$\delta\sigma_{xx}^{\text{DOS}}$	$\delta\sigma_{xx}^{7-10}$	$\delta\sigma_{xx}^{\text{tot}}$
I	$\frac{e^2}{16\epsilon} \frac{e^2}{8\pi^4} \ln \frac{1}{\epsilon}$	$\frac{e^2}{8(\epsilon-\gamma\phi)} \ln \frac{\epsilon}{\gamma\phi} - \frac{14\zeta(3)e^2}{\pi^4} \ln \frac{1}{\epsilon}$	$-\frac{14\zeta(3)e^2}{\pi^4} \ln \frac{1}{\epsilon}$	$\frac{e^2}{3\pi^2} \ln \ln \frac{1}{T_{c0}\tau} + O(\epsilon)$	$\frac{e^2}{16\epsilon} + \frac{e^2}{8(\epsilon-\gamma\phi)} \ln \frac{\epsilon}{\gamma\phi} + \frac{e^2}{3\pi^2} \ln \ln \frac{1}{T_{c0}\tau}$
I-III	$\frac{e^2}{2\epsilon} \left(\frac{\epsilon}{2h}\right)^2 \left[\psi\left(\frac{1}{2} + \frac{\epsilon}{2h}\right) - \psi\left(\frac{\epsilon}{2h} - \frac{h}{\epsilon}\right)\right]$	$\frac{e^2}{8\epsilon-\gamma\phi} \left[\psi\left(\frac{1}{2} + \frac{t\epsilon}{2h}\right) - \psi\left(\frac{1}{2} + \frac{t\gamma\phi}{2h}\right)\right] - \frac{14\zeta(3)e^2}{\pi^4} \left[\ln\left(\frac{t}{2h}\right) - \psi\left(\frac{1}{2} + \frac{t\epsilon}{2h}\right)\right]$	$-\frac{14\zeta(3)e^2}{\pi^4} \left[\ln\left(\frac{t}{2h}\right) - \psi\left(\frac{1}{2} + \frac{t\epsilon}{2h}\right)\right]$	$\frac{e^2}{3\pi^2} \ln \ln \frac{1}{T_{c0}\tau} + O(\max[\epsilon, h^2])$	
IV	$\frac{4e^2\gamma_E^2 t^2}{3\pi^2 h^2}$	$-\frac{2e^2}{\pi^2} \ln \frac{1}{h} - \frac{2\gamma_E e^2}{\pi^2} \left(\frac{t}{h}\right)$	$-\frac{4e^2\gamma_E^2 t^2}{3\pi^2 h^2}$	$\frac{4e^2}{3\pi^2} \ln \frac{1}{h}$	$-\frac{2e^2}{3\pi^2} \left(\ln \frac{1}{h} + \frac{3t}{h}\right)$
V	$\frac{2\gamma_E e^2}{\pi^2} \left(\frac{t}{h}\right)$	$-\frac{2e^2}{3\pi^2} \ln \frac{1}{4\gamma_E t}$	$-\frac{2\gamma_E e^2}{\pi^2} \left(\frac{t}{h}\right)$	$\frac{4e^2}{3\pi^2} \ln \frac{1}{4\gamma_E t}$	$-\frac{2e^2}{3\pi^2} \ln \frac{1}{4\gamma_E t}$
VI-VII	$\frac{e^2}{4} \frac{t}{h-h_{c2}(t)}$	$-\frac{2e^2}{3\pi^2} \ln \frac{2h}{\pi^2 t}$	$-\frac{e^2}{4} \frac{t}{h-h_{c2}(t)}$	$\frac{4e^2}{3\pi^2} \ln \frac{2h}{\pi^2 t}$	$-\frac{2e^2}{3\pi^2} \ln \frac{h_{c2}(t)}{h-h_{c2}(t)}$
VIII	$\frac{e^2}{6\pi^2} \frac{C_1}{\ln 3 t}$	$-\frac{e^2}{\pi^2} \ln \frac{1}{\ln t} + \frac{\pi^2 e^2}{192} \frac{\ln \frac{\pi^2}{2\gamma\phi}}{\ln^2 t}$	$-\frac{\pi^2 e^2}{192} \frac{1}{\ln^2 t}$	$\frac{e^2}{3\pi^2} \ln \frac{1}{T_{c0}\tau} \frac{1}{\ln t}$	$-\frac{2e^2}{3\pi^2} \ln \frac{1}{T_{c0}\tau} \frac{1}{\ln t}$
IX	$\frac{\pi^2 e^2}{192} \left(\frac{t}{h}\right)^2 \frac{C_2}{\ln^3 \frac{2h}{\pi^2}}$	$-\frac{e^2}{\pi^2} \ln \frac{1}{\ln \frac{2h}{\pi^2}} + \frac{7\zeta(3)\pi^2 e^2}{768} \left(\frac{t}{h}\right)^2 \frac{1}{\ln^2 \frac{2h}{\pi^2}}$	$-\frac{7\zeta(3)\pi^2 e^2}{384} \left(\frac{t}{h}\right)^2 \frac{1}{\ln^2 \frac{2h}{\pi^2}}$	$\frac{e^2}{3\pi^2} \ln \frac{1}{\ln \frac{2h}{\pi^2}} \frac{1}{\ln \frac{2h}{\pi^2}}$	$-\frac{2e^2}{3\pi^2} \ln \frac{\ln \frac{1}{T_{c0}\tau}}{\ln \frac{2h}{\pi^2}} - \frac{7\zeta(3)\pi^2 e^2}{768} \left(\frac{t}{h}\right)^2 \frac{1}{\ln^2 \frac{2h}{\pi^2}}$

TABLE I. Asymptotic expressions in different domains, shown in Fig. 5. The first column gives the domain according to that figure and is determined by the t & h regions given in table II.

domain	t and h range	description
I	$h = 0, \epsilon \ll 1$	zero field, near T_{c0}
II	$h - h_{c2} \sim \epsilon \ll 1$	near T_{c0} -reflected h_{c2} -line
III	$h - h_{c2}(t) \ll 1, \epsilon \ll 1$	near h_{c2} -line
I - III	$h \ll 1, \epsilon \ll 1$	full GL region
IV	$t \ll h - h_{c2}(t)$	region of QFs
V	$\tilde{h} \sim t \ll 1$	quantum-to-classical
VI	$\tilde{h} \lesssim t \ll 1$	classical, near $h_{c2}(t \rightarrow 0)$
VII	$h - h_{c2}(t) \lesssim t \ll h_{c2}(t)$	classical, strong fields
VIII	$\ln t \gtrsim 1, h \ll t$	high temperatures
IX	$h \gg \max\{1, t\}$	high magnetic fields

TABLE II. Explanation of the different domains with t & h ranges. Here $\epsilon = \ln t$.

The most surprising result in table I is the domain IV, the region of quantum fluctuations (see Fig. 3): one sees that the positive AL (the anomalous MT contribution is equal to the AL one in that domain) decays with decreasing temperature as T^2 . Moreover, it is exactly cancelled by the negative contribution of the four DOS-like diagrams 3-6:

$$\delta\sigma_{xx}^{\text{AL}} = \delta\sigma_{xx}^{\text{MT(an)}} = -\delta\sigma_{xx}^{\text{DOS}} = \frac{4e^2\gamma_E^2 t^2}{3\pi^2 h^2}. \quad (4)$$

The total fluctuation contribution to conductivity $\delta\sigma_{xx}^{(\text{tot})}$ in this important region ($t \ll \tilde{h}$) is *completely determined by the renormalization of the diffusion coefficient* (the regular part of the MT contribution and diagrams 7-10). It turns out to be negative and at zero temperature diverges logarithmically when the magnetic field approaches $H_{c2}(0)$. The non-trivial fact following from Eq. (3) is that an increase of temperature at a fixed value of the magnetic field in this domain mainly results in a

further decrease of conductivity

$$\delta\sigma_{xx}^{(\text{tot})} = -\frac{2e^2}{3\pi^2} \ln \frac{1}{\tilde{h}} - \frac{6\gamma_E e^2 t}{\pi^2} \frac{1}{\tilde{h}} + O\left[\left(\frac{t}{\tilde{h}}\right)^2\right], \quad (5)$$

and only at the boundary with domain V, when $t \sim \tilde{h}$, the total fluctuation contribution $\delta\sigma_{xx}^{(\text{tot})}$ passes through a minimum and starts to grow. Such non-monotonic behavior of the conductivity close to $H_{c2}(0)$ was multiple times observed in experiments^{17,18} (see Fig. 9).

The domain V describes the transition regime between quantum and classical fluctuations, while in the domains VI-VII, extended along the line $H_{c2}(T)$, superconducting fluctuations have already classical (but non-Ginzburg-Landau) character. In all these three regions one observes exactly the same cancellation of the AL and DOS contributions as in domain IV and $\delta\sigma_{xx}^{(\text{tot})}$ is determined by the negative DCR contribution.

Finally, in the peripheral domains VIII-IX, the direct positive contribution of fluctuation Cooper pairs (AL) to conductivity decays faster than all the other: $\sim \ln^{-3}(T/T_{c0})$. We stress, that this exact result differs from the evaluation of the AL paraconductivity far from the transition of Ref. [7], but is in complete agreement with the high temperature asymptotic expression for the paraconductivity of a clean 2D superconductor, see Ref. [19]. This agreement seems natural: fluctuation Cooper pair transport is insensitive to impurity scattering. The anomalous MT contribution, in complete accordance with Refs. [7 and 8], decays as $\sim \ln \gamma_\phi^{-1} / \ln^{-2}(T/T_{c0})$. The contribution of diagrams 3-6 also decays as $\ln^{-2}(T/T_{c0})$, but without the large factor $\ln \gamma_\phi^{-1}$. Finally, the regular MT contribution together with the ones from diagrams 7-10 decay extremely slow, in fact double logarithmically:

$$\delta\sigma_{xx}^{(\text{DCR})} = -\frac{2e^2}{3\pi^2} \left(\ln \ln \frac{1}{T_{c0}\tau} - \ln \ln \frac{T}{T_{c0}} \right). \quad (6)$$

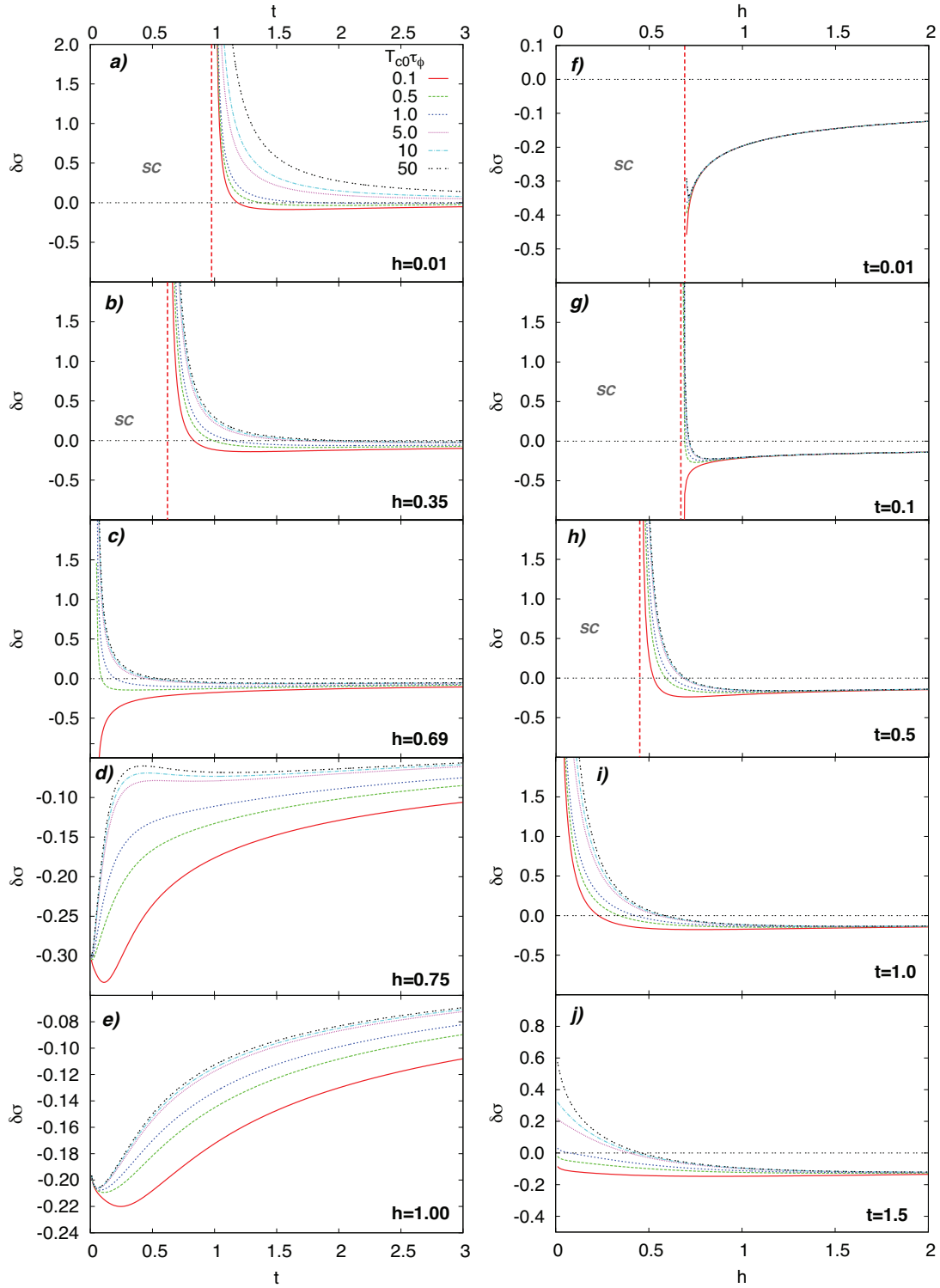


FIG. 6. (Color online) Total fluctuation conductivity for different $T_{c0}\tau_{\phi}$ for several constant temperatures t and magnetic fields h . a) to e) show $\delta\sigma(t)$ for different magnetic fields below ($h = 0.01, 0.35$, superconducting region marked by "SC"), at ($h = 0.69$), and above ($h = 0.75, 1.0$) the zero temperature critical field $H_{c2}(0)$. The legend key of a) applies to all panels. Note, that the value of $T_{c0}\tau_{\phi}$ near the transition at $t = 0$ can determine the sign of the fluctuation conductivity - however at very low temperatures the FC becomes independent of the phase-breaking time and all lines coalesce which is not resolved in that plot. f) to j) show $\delta\sigma(h)$ for constant temperatures, below ($t = 0.01, 0.1, 0.5$), at ($t = 1.0$), and above ($t = 1.5$) the transition temperature T_{c0} . All plots are calculated for $T_{c0}\tau = 10^{-3}$. If $\delta\sigma = 0$ is within plot range, it is marked by a horizontal dashed line, and the critical magnetic fields $H_{c2}(T)$ are shown as (red) vertical dashed lines. See detailed discussion in the text.

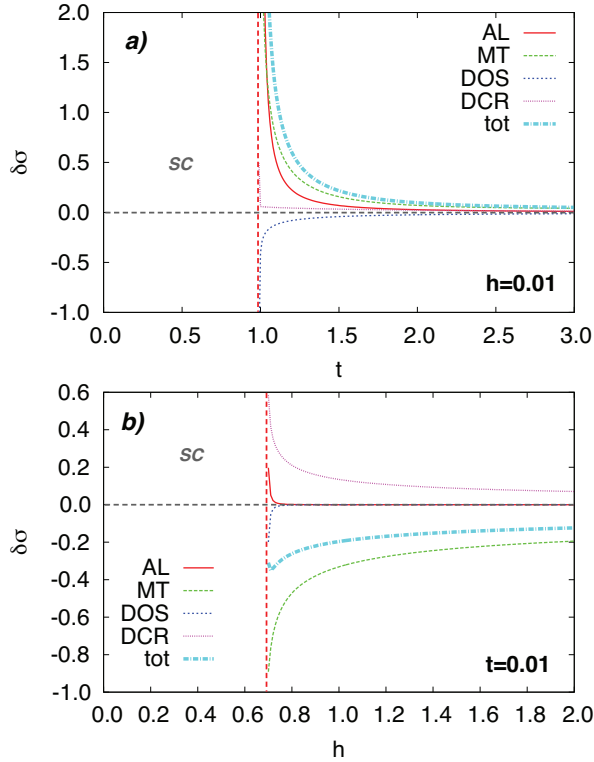


FIG. 7. (Color online) Fluctuation conductivity contributions: AL, MT, DOS, DCR, and total (tot) for $T_{c0}\tau = 10^{-3}$ and $T_{c0}\tau_\phi = 5$. a) shows the temperature dependence at low field $h = 0.01$, and b) the field dependence at low temperature $t = 0.01$.

Up to the numerical prefactor this expression coincides with the results of Ref. [7 and 9].

Eq. (3) provides the basis for a “fluctuoscope” for superconductors, i.e. the extraction of its microscopic parameters from the analysis of fluctuation corrections. Indeed one can see that $\delta\sigma_{xx}^{(\text{tot})}$ depends on two superconducting parameters: $T_{c0}, H_{c2}(0)$, the elastic scattering time τ , and (temperature dependent) phase-breaking time $\tau_\phi(T)$. The elastic scattering time can be obtained from the normal state properties of the superconductor, while the Eq. (3) can become the instrument for the precise determination of the critical temperature T_{c0} (instead of the often used rule “half width of transition”) and $H_{c2}(0)$. Moreover, it can be an invaluable tool for the study of the temperature dependence of the phase-breaking time $\tau_\phi(T)$.

The exemplary surface of $\delta\sigma_{xx}^{(\text{tot})}(T, H)$ presented in Fig. 2 for $T_{c0}\tau = 10^{-2}$ and $T_{c0}\tau_\phi = 10$ shows that the value of τ_ϕ determines the behavior of fluctuation corrections only in the region of low fields. It is convenient to analyze Fig. 2 side-by-side with Fig. 3 where lines $\delta\sigma_{xx}^{(\text{tot})}(T, H) = \text{const}$ through the phase diagram are shown. It is interesting to note that the numerical analysis of Eq. (3) shows that the logarithmic asymp-

totic Eq. (5) is valid only within an extremely narrow field range $\tilde{h} \lesssim 10^{-6}$.

In order to get a broader overview of the richness of our main result, we compiled several magneto-conductivity single-parameter dependencies (cuts through the “surface” at constant t or h) in Fig. 6. Each individual panel a) through j) of this figure shows the total FC for six different values of $T_{c0}\tau_\phi$ between 0.1 and 50 and fixed $T_{c0}\tau = 10^{-3}$. If $\delta\sigma = 0$ is within plot range, it is marked by a horizontal dashed line, and the critical magnetic fields $H_{c2}(T)$ are shown as (red) vertical dashed lines. a) to e) show $\delta\sigma(t)$ for different magnetic fields below ($h = 0.01, 0.35$, superconducting region marked by “SC”), at ($h = 0.69$), and above ($h = 0.75, 1.0$) the zero temperature critical field $H_{c2}(0)$. The legend key of a) applies to all panels. The behavior is as expected from the above discussion, but it is very educative to take a closer look at the behavior near the QPT [panel c)]: As mentioned above, the asymptotic expression for the quantum regime is only valid at extremely small temperatures, which cannot be resolved in this plot. Therefore one sees in particular for the smallest $T_{c0}\tau_\phi$ -value a sharp dip in the FC at low temperatures, which will eventually coalesce with all other curves at even lower temperature (not visible) and become independent of the phase-breaking time, as can be seen at larger h in panel d) and e).

f) to j) show $\delta\sigma(h)$ for constant temperatures, below ($t = 0.01, 0.1, 0.5$), at ($t = 1.0$), and above ($t = 1.5$) the transition temperature T_{c0} . Here again, it is seen in panel f) that in the quantum regime the FC is mostly independent of the phase-breaking time and only close to the QPT a separation of the curves becomes visible since even the small temperature $t = 0.01$ becomes of order \tilde{h} or even larger and the asymptotic expression does not hold anymore.

In Fig. 7 we plotted two particular curves of Fig. 6 in more detail, showing the different contributions from the diagram groups a)-d) of Fig. 1. These are the curves for $T_{c0}\tau_\phi = 5$ at lowest magnetic field $h = 0.01$ [in a)] and temperature $t = 0.01$ [in b)]. Comparing these curves to the asymptotics of table I, one sees, that the behavior near T_{c0} is as expected [see a)], and in particular the contribution from diagrams 7-10 is negligible. However, in the quantum regime it becomes the dominating contribution, rendering the total FC negative and only close to the QPT is cancelled by the MT contribution.

Despite Eq. (3) being a closed expression, its specific evaluation in the most general case requires sophisticated numerical summation and integration. While being straight-forward, one might encounter technical difficulties in the evaluation of the complex Poly-Gamma functions $\psi^{(n)}(z)$. Moreover, the summation cut-off parameter M can reach extremely large values at low temperatures [experimental values $(T_{c0}\tau)_{\text{exp}}^{-1}$ for materials near the superconductor-insulator transition can be on the order 10^6], which slows down the numerical procedure significantly. The latter difficulty can be partially overcome

by evaluation of the slowly divergent tails of the m -sums in Eq. (3) as integrals. Here, we should also note that for fitting purposes one does not need to choose the real, often extremely small, experimental values $(T_{c0}\tau)_{\text{exp}}$. To save CPU time, one can assume the value $(T_{c0}\tau)_{\text{num}}$ of this parameter to be much larger than $(T_{c0}\tau)_{\text{exp}}$ (but still much less than $T_{c0}\tau_{\phi}$) and only at the very end to shift the final expression by $\ln \frac{(T_{c0}\tau)_{\text{num}}}{(T_{c0}\tau)_{\text{exp}}}$. Nevertheless, the numerics of the problem remains challenging: for the surface plot in Fig. 2 we evaluated 10^6 values for $\delta\sigma$ with the modest assumption $(T_{c0}\tau)_{\text{num}} = 0.01$, yet it still took three month of single CPU time for its calculation. Our optimized tool for the evaluation of Eq. (3) can be found at [16].

IV. COMPARISON WITH EXPERIMENTAL RESULTS

A main aspect of this work is, that the complete expression, Eq. 3, can be used to extract experimental parameters of thin superconducting films from measured data ("fluctuoscropy"). In particular the critical temperature T_{c0} , the critical magnetic field $H_{c2}(0)$, and the phase-breaking time τ_{ϕ} .

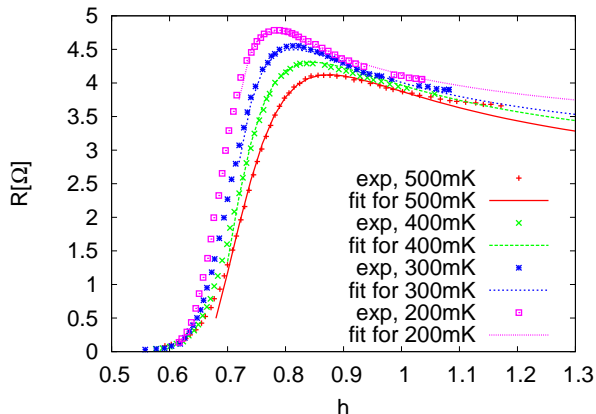


FIG. 8. (Color online) Comparison to resistivity measurements in thin indium oxide films, published in Ref. [20]. Here we present the data taken from Fig. 4a of [20] for the "Weak" sample with thickness 30nm, $T_{c0} = 3.35\text{K}$, and $B_{c2}(0) = 13\text{T}$. We fitted the resistivity R for temperatures 0.2, 0.3, 0.4, and 0.5K using our full expression for $\delta\sigma$ with the experimentally found T_{c0} . For $B_{c2}(0)$ we fitted a slightly larger value of 13.7T and $T_{c0}\tau_{\phi} = 5 \pm 1$.

As an example of the practical use for our results, we fitted two different sets of experimental data. First we compared our general Eq. (3) to resistivity measurements in thin disordered indium oxide films, presented in Ref. [20]. Figure 8 shows the low temperature data for one sample (referred to as "Weak" in Ref. [20]) of a film with thickness 30nm, transition temperature $T_{c0} = 3.35\text{K}$

and critical magnetic field $B_{c2}(0) = 13\text{T}$. The resistivity was measured, depending on magnetic field, for low temperature values $T = 200, 300, 400, 500\text{mK}$. We plotted the theoretical expression for $\delta\sigma_{xx}^{(\text{tot})}$ using the fitting parameter values $B_{c2}(0) = 13.7\text{T}$, $T_{c0}\tau_{\phi} = 5 \pm 1$, and the experimentally found value of $T_{c0} = 3.35\text{K}$. Overall the fitted FC curves show good agreement with the results of the measurements.

Second we re-analyzed data for thin films of the compound $\text{La}_{2-x}\text{Ce}_x\text{CuO}_4$, with $x = 0.09$, in high magnetic fields, see Ref. [17]a, with thickness 100nm. In contrast to the indium oxide film, we fitted the temperature dependence of the FC at different constant high magnetic fields here. This sample has $T_{c0} \approx 22.5\text{K}$ and we fitted $B_{c2}(0) \approx 6\text{T}$, which the 4T data suggests. In Fig. 9 we plotted the temperature dependence of Eq. (3) for different magnetic fields for fixed $T_{c0}\tau_{\phi} = 0.5$ and $T_{c0}\tau = 10^{-3}$.

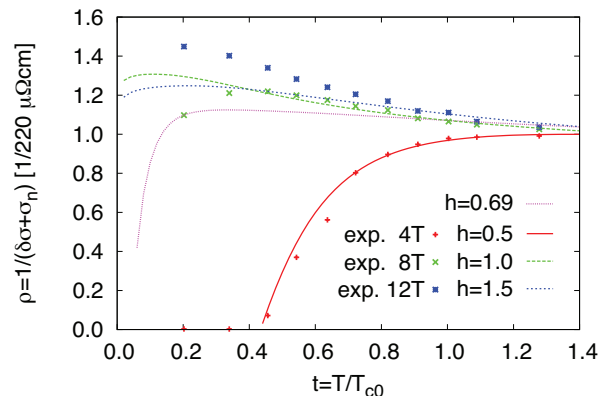


FIG. 9. (Color online) Temperature dependence of the FC at different fields close to $H_{c2}(0)$ and comparison to experimental data for a thin film of $\text{La}_{2-x}\text{Ce}_x\text{CuO}_4$ ($x = 0.09$) with $T_{c0} \approx 22.5\text{K}$ and fitted $B_{c2}(0) \approx 6\text{T}$ (see Fig. 1a of Ref. [17]a). For the theoretical curves a fixed $T_{c0}\tau_{\phi} = 0.5$ is used which nevertheless, captured the overall behavior. All curves are numerically calculated with $T_{c0}\tau = 10^{-3}$. The highest field curve could be possible fitted better, using a smaller τ_{ϕ} . However, as described in the text, τ_{ϕ} is in general temperature dependent and the available data does not allow to extract this values.

At this point it is important to remark, that τ_{ϕ} depends on temperature in general, such that for a better fit one needs first to analyze FC data at constant temperatures to extract $\tau_{\phi}(T)$ and then fit temperature dependent data. This way one can obtain precise values for the otherwise difficult to determine experimental parameters T_{c0} , $H_{c2}(0)$, and $\tau_{\phi}(T)$. However, the data of Ref. [17]a does not allow to extract this information for a better fit in Fig. 9.

V. QUANTUM LIQUID OF FCP IN THE VICINITY OF $H_{c2}(0)$.

An analysis of the obtained results allows us to offer a qualitative picture of the quantum phase transition (QPT) occurring in the vicinity of $H_{c2}(0)$ at very low temperatures. Above we presented the complete microscopic calculation. However, it is instructive to start our discussion of the QFs by describing and refreshing the qualitative picture of SFs in the vicinity of T_{c0} , in the Ginzburg-Landau region¹, for further comparison. In domains I- III, the lifetime of fluctuation-induced Cooper pairs τ_{GL} can be obtained in the simplest way by using the uncertainty principle. Indeed, $\tau_{GL} \sim \hbar/\Delta E$, where ΔE is the energy difference $k_B(T - T_{c0})$ ensuring that τ_{GL} should become infinite at the transition point. This yields the standard Ginzburg-Landau time

$$\tau_{GL} \sim \hbar/k_B(T - T_{c0}) \sim \hbar/(k_B T_{c0} \epsilon), \quad (7)$$

where $\epsilon = (T - T_{c0})/T_{c0} \ll 1$ is the reduced temperature. In its turn the coherence length $\xi_{GL}(T)$ can be estimated as the distance, which two electrons move apart during the GL time:

$$\xi_{GL}(\epsilon) = (\mathcal{D}\tau_{GL})^{1/2} \sim \xi_{BCS}/\sqrt{\epsilon}.$$

Here $\xi_{BCS} \sim \sqrt{\mathcal{D}/T_{c0}}$ is the BCS coherence length, \mathcal{D} is the diffusion coefficient. The fluctuating order parameter $\Delta^{(fl)}(\mathbf{r}, t)$ varies close to T_{c0} on a larger scale $\xi_{GL}(\epsilon) \gg \xi_{BCS}$. The ratio of the FCP concentration to the corresponding effective mass with logarithmic accuracy can be estimated as $n_{c.p.}/m_{c.p.} \sim \xi_{GL}^{2-D}(\epsilon)$ and in the 2D case assume as constant (which is the case we will discuss in the following)¹.

The two principal fluctuation contributions to conductivity close to T_{c0} , are positive and originate from a direct FCP charge transfer (AL contribution)

$$\delta\sigma_{xx}^{AL} \sim (n_{c.p.}/m_{c.p.}) e^2 \tau_{GL} \sim e^2/\hbar\epsilon \quad (8)$$

and from the specific quantum process of one-electron charge transfer related to coherent scattering of electrons on elastic impurities, which leads to the formation of FCPs (anomalous MT contribution)

$$\delta\sigma_{xx}^{MT(an)} \sim \frac{e^2}{\hbar\epsilon} \ln(\epsilon/\gamma_\phi).$$

However, these two contributions do not capture the complete effect of fluctuations on conductivity. The involvement of quasi-particles in the fluctuation pairing results in their absence at the Fermi level, i.e., in the opening of a pseudo-gap in the one-electron spectrum and consequently decrease the one-particle Drude-like conductivity. Such an indirect effect of the FCP formation is usually referred as the DOS contribution. Being proportional to the concentration of the FCPs $n_{c.p.}$, the DOS contribution formally appears by integration

of the Fourier-component $\langle |\Delta^{(fl)}(\mathbf{q}, \omega)|^2 \rangle$ of the order parameter over all long-wave-length fluctuation modes ($q \lesssim \xi_{BCS}^{-1} \sqrt{\epsilon}$); in the static approximation ($\omega \rightarrow 0$) given by:

$$\delta\sigma_{xx}^{DOS} \sim -\frac{2n_{c.p.}e^2\tau}{m_e} \sim -e^2 \int \frac{\xi_{BCS}^2 d^2\mathbf{q}}{\epsilon + \xi_{BCS}^2 q^2} \sim -\frac{e^2}{\hbar} \ln \frac{1}{\epsilon}. \quad (9)$$

One sees that the DOS contribution has the opposite sign with respect to the AL and MT contributions, but close to T_{c0} does not compete with those, since it turns out to be less singular as a function of temperature.

Finally, the one-electron diffusion coefficient is renormalized in the presence of fluctuation pairing (DCR). Close to T_{c0} this contribution is not singular in ϵ (see table I) and was usually ignored in literature, but as was mentioned before, it becomes of primary importance relatively far from T_{c0} , and at very low temperatures. It is due to $\delta\sigma_{xx}^{DCR}$ that the sign of the total contribution of fluctuations to conductivity $\delta\sigma_{xx}^{(tot)}$ changes in a wide domain of the phase diagram and in particular close to $T = 0$, in the region of quantum fluctuations (see Fig. 3, where the regions with dominating fluctuation contributions to magneto-conductivity are shown).

At zero temperature and fields above $H_{c2}(0)$, the systematics of the fluctuation contributions to the conductivity changes considerably with respect to that close to T_{c0} . Due to the collision-less rotation of FCPs (they do not "feel" the presence of elastic impurities, all information concerning electron scattering is already included in the effective mass of the Cooper pairs) they do not contribute directly to the longitudinal (along the applied electric field) electric transport (analogously to the suppression of the one-electron conductivity in strong magnetic fields ($\omega_c\tau \gg 1$): $\delta\sigma_{xx}^{(e)} \sim (\omega_c\tau)^{-2}$, see Ref. [21]) and the AL contribution to $\delta\sigma_{xx}^{(tot)}$ becomes zero. The anomalous MT and DOS contributions tend to zero as well but because of different reasons. Namely, the former vanishes since magnetic fields as large as $H_{c2}(0)$ completely destroy the phase coherence, whereas the latter disappears since magnetic field suppresses the fluctuation gap in the one-electron spectrum. Therefore the effect of fluctuations on the conductivity at zero temperature is reduced to the renormalization of the one-electron diffusion coefficient. FCPs in the quantum region occupy the lowest Landau level, but all dynamic fluctuations in the frequency interval from 0 to Δ_{BCS} have to be taken into account. The corresponding fluctuation propagator at zero temperature close to $H_{c2}(0)$ has the form (see Eq. (A22))

$$L_0(\omega) = -\nu_0^{-1} \frac{1}{\hbar + \omega/\Delta_{BCS}}$$

and

$$\delta\sigma_{xx}^{DCR} \sim -\frac{e^2}{\Delta_{BCS}} \int_0^{\Delta_{BCS}} \frac{d\omega}{\hbar + \frac{\omega}{\Delta_{BCS}}} \sim -\frac{e^2}{\hbar} \ln \frac{1}{\hbar}. \quad (10)$$

The parameter $\tilde{h} = [H - H_{c2}(0)]/H_{c2}(0)$ plays the same role as the reduced temperature ϵ in the case of the classical transition; Δ_{BCS} is the BCS value of the gap at zero temperature in zero field.

While the denominator of the integrand in Eq. (9) defines the characteristic wavelength $\xi_{\text{GL}}(T)$ of the fluctuation modes close to T_{c0} , the one in Eq. (10) defines the characteristic coherence time $\tau_{\text{QF}}(\tilde{h})$ of QFs near $H_{c2}(0)$ (where $t \ll \tilde{h}$). The value of the integral is determined by its lower cut-off $\omega_{\text{QF}} \sim \Delta_{\text{BCS}}\tilde{h}$, and the corresponding time scale is

$$\tau_{\text{QF}} \sim \hbar \left(\Delta_{\text{BCS}}\tilde{h} \right)^{-1}. \quad (11)$$

One sees that the functional form of τ_{QF} is completely analogous to that of τ_{GL} : $\Delta_{\text{BCS}} \triangleq T_{c0}$ and the reduced field \tilde{h} plays the role of reduced temperature ϵ . Eq. (11) can also be obtained from the uncertainty principle. Indeed, the energy, characterizing the proximity to the quantum phase transition is $\Delta E = \hbar\omega_c(H) - \hbar\omega_c(H_{c2}(0)) \sim \Delta_{\text{BCS}}\tilde{h}$ and namely this value should be used in the Heisenberg relation instead of $k_B(T - T_{c0})$, as was done in the vicinity of T_{c0} . The spatial coherence scale $\xi_{\text{QF}}(\tilde{h})$ can be estimated from the value of τ_{QF} analogously to the consideration near T_{c0} . Namely, two electrons with coherent phase starting from the same point get separated by the distance

$$\xi_{\text{QF}}(\tilde{h}) \sim (D\tau_{\text{QF}})^{1/2} \sim \xi_{\text{BCS}}/\sqrt{\tilde{h}},$$

after time τ_{QF} .

To clarify the physical meaning of τ_{QF} and ξ_{QF} , note that near the quantum phase transition at zero temperature, where $H \rightarrow H_{c2}(0)$, the fluctuations of the order parameter $\Delta^{(\text{fl})}(\mathbf{r}, t)$ become highly inhomogeneous, contrary to the situation near T_{c0} . Indeed, below $H_{c2}(0)$, the spatial distribution of the order parameter at finite magnetic field reflects the appearance of Abrikosov vortices with average spacing [close to $H_{c2}(0)$ but in the region where the notion of vortices is still adequate] equal to

$$a(H) = \xi_{\text{BCS}}/\sqrt{H/H_{c2}(0)} \rightarrow \xi_{\text{BCS}}.$$

Therefore, one expects that close to and above $H_{c2}(0)$ the fluctuation order parameter $\Delta^{(\text{fl})}(\mathbf{r}, t)$ also has a "vortex-like" spatial structure and varies over the scale ξ_{BCS} and being preserved over time τ_{QF} . In the language of FCPs, one describes this situation in the following way: A FCP at zero temperature and in magnetic field close to $H_{c2}(0)$ rotates with Larmor radius $r_L \sim v_F/\omega_c(H_{c2}(0)) \sim v_F/\Delta_{\text{BCS}} \sim \xi_{\text{BCS}}$, which represents its effective size. During time τ_{QF} two initially selected electrons participate in multiple fluctuating Cooper pairings maintaining their coherence. The coherence length $\xi_{\text{QF}}(\tilde{h}) \gg \xi_{\text{BCS}}$ is thus a characteristic size of a cluster of such coherently rotating FCP, and τ_{QF} estimates the

lifetime of such a *flickering* cluster. One can view the whole system as an ensemble of flickering domains of coherently rotating FCP, precursors of vortices (see Fig. 4).

In view of the qualitative picture of SFs in the regime of the QPT, let us continue with the scenario of Abrikosov lattice defragmentation: Approaching $H_{c2}(0)$ from below, puddles of fluctuating vortices are formed, which are nothing else as FCPs rotating in a magnetic field. Their characteristic size is $\xi_{\text{QF}}(\tilde{h})$, and they flicker in the characteristic time $\tau_{\text{QF}}(\tilde{h})$. In this situation, the supercurrent can still flow through the sample until these puddles do not break the last percolating superconductive channel. The corresponding field determines the value of the by QFs renormalized second critical field: $H_{c2}^*(0) = H_{c2}(0) [1 - 2\text{Gi} \ln(1/\text{Gi})]$ (see Ref. [1]). Above this field no supercurrent can flow through the sample anymore, i.e., the system is in the normal state. Nevertheless, as demonstrated by the above estimates, its properties are strongly affected by the QF. Fragments of the Abrikosov lattice can be still observed in this region by the following Gedanken experiment: The clusters of rotating FCP ("ex-vortices") of size ξ_{QF} with some kind of the superconducting order should be found in the background of the normal state, if one takes a picture with exposure time shorter than τ_{QF} . For exposure times longer than τ_{QF} , the picture is smeared out and no traces of the Abrikosov vortex state can be found. However, the detailed nature of the order which exists there is still unclear. It would be attractive to identify these clusters with fragments of the Abrikosov lattice, but most probable this is some kind of quantum FCP liquid. Indeed, the presence of structural disorder can result in the formation of a hexatic phase close to $H_{c2}^*(0)$, where the translational invariance no longer exists, while at the same time conserving the orientational order or the vortices.

VI. DISCUSSION

In terms of the introduced QF characteristics τ_{QF} and ξ_{QF} , one can understand the meaning of already found microscopic QF contributions to different physical values in the vicinity of $H_{c2}(0)$ and derive others which are related.

A. In-plane conductivity

For example, the physical meaning of Eq. (4) can be understood as follows: one could estimate the FCP conductivity by merely replacing $\tau_{\text{GL}} \rightarrow \tau_{\text{QF}}$ in the classical AL expression (8), which would give $\delta\tilde{\sigma}^{AL} \sim e^2\tau_{\text{QF}}$. Nevertheless, as we already noticed, a FCP at zero temperature cannot drift along the electric field but only rotates around a fixed center. As temperature deviates from zero, FCPs can change their state due to the interaction with the thermal bath, i.e. their hopping to

an adjacent rotation trajectory along the applied electric field becomes possible. This means that FCP can participate in longitudinal charge transfer now. This process can be mapped onto the paraconductivity of a granular superconductor²² at temperatures above T_{c0} , where the FCP tunneling between grains occurs in two steps: first one electron jumps, then the second follows. The probability of each hopping event is proportional to the inter-grain tunneling rate Γ . To conserve the superconducting coherence between both events, the latter should occur during the FCP lifetime τ_{GL} . The probability of FCPs tunneling between two grains is determined by the conditional probability of two one-electron hopping events and is proportional to $W_{\Gamma} = \Gamma^2 \tau_{\text{GL}}$. Coming back to the situation of FCPs above $H_{c2}(0)$, one can identify the tunneling rate with temperature T while τ_{GL} corresponds to τ_{QF} . Therefore, in order to obtain a final expression, $\delta\tilde{\sigma}^{\text{AL}}$ should be multiplied by the probability factor $W_{\text{QF}} = t^2 \tau_{\text{QF}}$ of the FCP hopping to the neighboring trajectory:

$$\delta\sigma_{xx}^{\text{AL}} \sim \delta\tilde{\sigma}^{\text{AL}} W_{\text{QF}} \sim e^2 t^2 / \tilde{h}^2,$$

which corresponds to the asymptotic Eq. (4).

B. Magnetic susceptibility

In order to estimate the contribution of QFs to the fluctuation induced magnetic susceptibility of the SC in the vicinity of $H_{c2}(0)$, one can apply the Langevin formula to a coherent cluster of FCPs and identify its average size by the rotator radius. One finds

$$\chi^{\text{AL}} = \frac{e^2 n_{\text{c.p.}}}{m_{\text{c.p.}} c} \langle \xi_{\text{QF}}^2(\tilde{h}) \rangle \sim \xi_{\text{BCS}}^2 / c \tilde{h}$$

in complete agreement with the result of Ref. [15].

C. Nernst coefficient

One further reproduces the contribution of QFs to the Nernst coefficient. Close to $H_{c2}(0)$ the chemical potential of FCPs can be identified as $\mu_{\text{FCP}} = \hbar\omega_c(H_{c2}(0)) - \hbar\omega_c(H)$ [as in Ref. [13], close to T_{c0} , $\mu_{\text{FCP}} = k_{\text{B}}(T_{c0} - T)$]. The corresponding derivative is $d\mu_{\text{FCP}}/dT \sim dH_{c2}(T)/dT \sim -T/\Delta_{\text{BCS}}$. Using the relation between the latter and the Nernst coefficient, it is possible to reproduce one of the results of Ref. [13]:

$$\nu^{\text{AL}} \sim [\tau_{\text{QF}}/m_{\text{c.p.}}] d\mu_{\text{FCP}}/dT \sim \xi_{\text{BCS}}^2 t / \tilde{h}.$$

D. Transversal magneto-resistance above $H_{c2}(0)$

The proposed qualitative approach can also explain the non-monotonic behavior of the transversal magneto-

resistance observed in the *layered* organic superconductor $\kappa - (\text{BEDT} - \text{TTF})_2\text{Cu}(\text{NCS})_2$ above $H_{c2}(0)$ at low temperatures²³. Indeed, the motion of FCPs along the z-axis in such a system has hopping character and the quasi-particle spectrum can be assumed to have the form of a corrugated cylinder. Close to T_{c0} the fluctuation magneto-conductivity tensor in this model was already studied in details in Ref. [6]. There it was demonstrated that the transverse paraconductivity in that case is suppressed by the square of the small anisotropy parameter $(\xi_z/\xi_x)^2$, while the dependence on the reduced temperature ϵ is even more singular than in plane. In terms of the Ginzburg-Landau FCP life-time (7), it can be written as

$$\delta\sigma_{zz}^{\text{AL}}(\epsilon) = \frac{4e^2\xi_z^4}{\pi^2\xi_x^2s^3} T_{c0}^2 \tau_{\text{GL}}^2(\epsilon), \quad (12)$$

where s is the interlayer distance. In principle this result could be obtained, even from the Drude formula applied to the FCP charge transfer [see above, how Eq. (8) for $\delta\sigma_{xx}^{\text{AL}}(\epsilon)$ was obtained] combined with the above speculations regarding the hopping of FCPs along z-axis²². This general approach, which does not involve the GL scheme, allows us to map Eq. (12) on the case of the QPT by just replacing $\tau_{\text{GL}}(\epsilon) \rightarrow \tau_{\text{QF}}(\tilde{h})$:

$$\delta\sigma_{zz}^{\text{AL}}(\tilde{h}) = \frac{4e^2\xi_z^4}{\xi_x^2s^3} T_{c0}^2 \tau_{\text{QF}}^2(\tilde{h}) = \frac{4e^2\xi_z^4}{\xi_x^2s^3} \left(\frac{\gamma E}{\pi}\right)^2 \frac{1}{\tilde{h}^2}.$$

The negative contribution appearing from the diffusion coefficient renormalization competes with the positive $\delta\sigma_{zz}^{\text{AL}}(\tilde{h})$. The only difference between the in-plane [see Eqs. (5) & (10)] and z-axis components of this one-particle contribution consists in the anisotropy factor $\langle v_z^2 \rangle / \langle v_x^2 \rangle = \xi_z^2 / \xi_x^2$. As a result one gets:

$$\delta\sigma_{zz}^{(\text{DCR})} = -\frac{2e^2}{3\pi^2s} \frac{\xi_z^2}{\xi_x^2} \ln \frac{1}{\tilde{h}}$$

and the total fluctuation correction to the z-axis magneto-conductivity at zero temperature above $H_{c2}(0)$ can be written as

$$\delta\sigma_{zz}^{(\text{tot})} = \frac{2e^2\xi_z^2}{3\pi^2\xi_x^2s} \left[1.94 \left(\frac{\xi_z}{s}\right)^2 \frac{1}{\tilde{h}^2} - \ln \frac{1}{\tilde{h}} \right]. \quad (13)$$

We used Eq. (13) for the analysis of unpublished data by M. Kartzovnik²³ on the magneto-resistance of the layered organic superconductor $\kappa - (\text{BEDT} - \text{TTF})_2\text{Cu}(\text{NCS})_2$ at low temperatures and magnetic fields above $H_{c2}(0)$. The measurement was taken at $T = 1.7\text{K}$ with a $T_{c0} \approx 9.5\text{K}$ and $B_{c2}(0) \approx 1.57\text{T}$ and this curve was fitted by $0.23 \left(0.18/\tilde{h}^2 + \ln \tilde{h}\right)$, see Fig. 10. For the material parameters of this compound, the author reports $\tau = 1.7\text{ps}$, $\xi_z = 0.3 - 0.4 \text{ nm}$, and $s = 1 \text{ nm}$. The fitting shown in Fig. 10 corresponds to the ratio $\xi_z/s = 0.32$ and looks rather convincing.

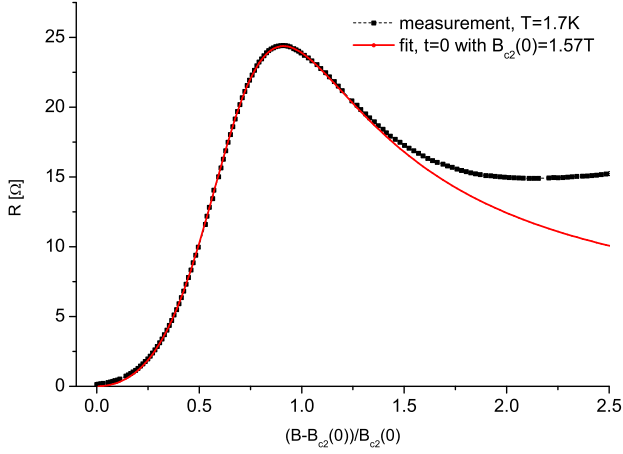


FIG. 10. (Color online) Comparison to resistivity measurements of the layered organic superconductor $\kappa - (BEDT - TTF)_2Cu(NCS)_2$ [23]. The material has a transition temperature of $T_{c0} \approx 9.5K$, $B_{c2}(0) \approx 1.57T$, and $\tau = 1.7ps$. This experimental curve is taken at $T = 1.7K$ and fitted by expression in Eq. (13), which is in perfect agreement with the experiment. Specifics are given in the text.

The discrepancy appearing between the theoretical and experimental curves in the high field region, M. Kartsovnik attributes to the large normal-state magneto resistance, reflecting the specifics of the cyclotron orbits on the multi-connected Fermi surface of the compound (due to the low crystal symmetry it is quite difficult to fit).

ACKNOWLEDGMENTS

We thank T. Baturina, Yu. Galperin, M. Kartsovnik, A. Koshelev, B. Leridon, and M. Norman for useful discussions. The work was supported by the U.S. Department of Energy Office of Science under the Contract No. DE-AC02-06CH11357. A.A.V. acknowledges support of the MIUR under the project PRIN 2008 and the European Community FP7-IRSES programs: "ROBOCON" and "SIMTECH".

Appendix A: Aslamazov-Larkin contribution

1. General expression

Let us start with the discussion of the AL contribution (diagram 1 in Fig. 1). The corresponding analytic

expression is

$$Q_{xx}^{AL}(\omega_\nu) = -4e^2T \sum_{\Omega_k} \sum_{\{n,m\}=0}^{\infty} \mathbf{B}_{nm}^{(x)}(\Omega_{k+\nu}, \Omega_k) L_m(\Omega_k) \times B_{mn}^{(x)}(\Omega_k, \Omega_{k+\nu}) L_n(\Omega_{k+\nu}). \quad (A1)$$

The block of three Green functions \mathbf{B}_{nm} with velocity operator (originating from the current vertex) and two Cooperons is given by

$$\mathbf{B}_{nm}(\Omega_{k+\nu}, \Omega_k) = T \sum_{\varepsilon_i} \text{Tr} \{ G(\varepsilon_i) \hat{\mathbf{v}} G(\varepsilon_{i+\nu}) \times \hat{\lambda}_n(\varepsilon_{i+\nu}, \Omega_{k-i}) G(\Omega_{k-i}) \hat{\lambda}_m(\Omega_{k-i}, \varepsilon_i) \}. \quad (A2)$$

The trace operator Tr denotes the integration over all electron quantum numbers. The corresponding block was calculated in [15] exactly for fields with $\omega_c \tau \ll 1$, i.e. for the case of our interest. Under this condition the Landau quantization affects the motion of Cooper pairs, while the Green functions in the block Eq. (A2) can be used in τ -approximation. As the result, using the properties of the velocity operator in Landau representation, one finds

$$B_{mn}^{(x)}(\Omega_{k+\nu}, \Omega_k) = -2\nu_0 \mathcal{D} \left[\sqrt{eH(n+1)} \delta_{m,n+1} + \sqrt{eHn} \delta_{m,n-1} \right] \Xi_{nm}(\Omega_{k+\nu}, \Omega_k), \quad (A3)$$

with

$$\Xi_{nm}(\Omega_k, \Omega_{k+\nu}) = 2\pi T \sum_{\varepsilon_i} \frac{\Theta(-\varepsilon_{i+\nu} \Omega_{k-i})}{|2\varepsilon_i + \omega_\nu - \Omega_k| + \omega_c(n+1/2)} \cdot \frac{\Theta(-\varepsilon_i \Omega_{k-i})}{|2\varepsilon_i - \Omega_k| + \omega_c(m+1/2)}. \quad (A4)$$

Substituting Eq. (A3) in Eq. (A1) and further summation over Landau levels in Eq. (A1), results in the cancellation of the terms containing the products $\delta_{m,n+1} \delta_{n,m+1}$ and $\delta_{m,n-1} \delta_{n,m-1}$. The analysis of the theta-functions in Eq. (A4) results in the possibility of separation of different domains of analyticity in the plane of bosonic frequencies Ω_k :

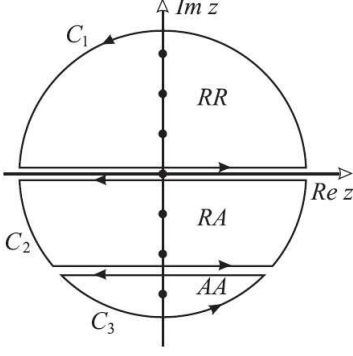


FIG. 11. The integration contour in the plane of complex frequencies.

$$\Xi_{mn}(\Omega_k, \Omega_k + \omega_\nu) = 2\pi T \left[\Theta(\Omega_k) \sum_{i=k}^{\infty} + \Theta(-\Omega_k) \sum_{i=0}^{\infty} + \Theta(-\Omega_k - \omega_\nu) \sum_{i=-\infty}^{k-1} + \Theta(\Omega_k + \omega_\nu) \sum_{i=-\infty}^{\nu-1} \right] \frac{1}{|2\varepsilon_i + \omega_\nu - \Omega_k| + \omega_c(n + 1/2)} \frac{1}{|2\varepsilon_i - \Omega_k| + \omega_c(m + 1/2)}. \quad (\text{A5})$$

Summation over fermionic frequency in this expression can already be performed in terms of ψ -functions:

$$\Xi_{mn}(\Omega_k, \Omega_k + \omega_\nu) = \frac{1}{2\omega_c(n-m)} \left[\psi\left(\frac{1}{2} + \frac{\omega_\nu + |\Omega_k| + \omega_c(n + 1/2)}{4\pi T}\right) - \psi\left(\frac{1}{2} + \frac{|\Omega_k| + \omega_c(m + 1/2)}{4\pi T}\right) + \psi\left(\frac{1}{2} + \frac{|\Omega_{k+\nu}| + \omega_c(n + 1/2)}{4\pi T}\right) - \psi\left(\frac{1}{2} + \frac{\omega_\nu + |\Omega_{k+\nu}| + \omega_c(m + 1/2)}{4\pi T}\right) \right]. \quad (\text{A6})$$

Being interested in the d.c. fluctuation conductivity, i.e. taking into account the limit $\omega_\nu \rightarrow -i\omega \rightarrow 0$ after analytical continuation, in Eq. (A6) we neglected the frequency ω_ν in comparison with $\omega_c(n-m)$ in denominator since the diagonal term ($m=n$) disappears in the process of summation over Landau levels in Eq. (A1) as follows from Eq. (A3). One notices the useful fact that the permutation $\Omega_k \Leftrightarrow \Omega_k + \omega_\nu$ simultaneously with $m \Leftrightarrow n$ in Eq. (A6) does not change the function $\Xi_{mn}(\Omega_k, \Omega_k + \omega_\nu)$:

$$\Xi_{mn}(\Omega_k, \Omega_k + \omega_\nu) \equiv \Xi_{nm}(\Omega_k + \omega_\nu, \Omega_k). \quad (\text{A7})$$

Let us return to the general expression for paraconductivity Eq. (A1). One can transform the sum over the bosonic frequencies Ω_k to the contour integral I^{AL} in the plane of complex frequency $\Omega_k \rightarrow -iz$:

$$Q_{xx}^{\text{AL}}(\omega_\nu) = -16e^2\nu_0^2\mathcal{D}^2eH \sum_{n,m} C_{mn} I_{nm}^{\text{AL}}(\omega_\nu), \quad (\text{A8})$$

$$I_{nm}^{\text{AL}}(\omega_\nu) = \frac{1}{4\pi i} \oint \coth\left(\frac{z}{2T}\right) dz \Xi_{nm}(-iz + \omega_\nu, -iz) \times \quad (\text{A9})$$

$$\Xi_{mn}(-iz, -iz + \omega_\nu) L_m(-iz) L_n(-iz + \omega_\nu),$$

where the contour integral encloses all frequencies Ω_k [in the plane of frequency z these are poles of $\coth(z/2T)$, see Fig. 11]. The coefficients

$$C_{mn} = (\delta_{m,n+1}\delta_{n,m-1} + \delta_{n,m+1}\delta_{m,n-1}) \sqrt{n}\sqrt{n+1} \quad (\text{A10})$$

control the summation over Landau levels.

Let us stress that both functions Ξ in Eq. (A9) have breaks of their analyticity along the lines $\text{Im}z = 0$ and $\text{Im}z = -\omega_\nu$, the same as the product of the propagators. As a result, one gets three domains where the integrand function is analytical: above the line $\text{Im}z = 0$, between the lines $\text{Im}z = 0$ and $\text{Im}z = -\omega_\nu$ and below $\text{Im}z = -\omega_\nu$. For the analytical continuation of function (A6) to the whole complex plane from Matsubara frequencies, three different functions: Ξ_{nm}^{RR} , Ξ_{nm}^{RA} , and Ξ_{nm}^{AA} , should be introduced, which are analytical in their corresponding domains. They differ by the combinations of the signs of

the explicit absolute values appearing in Eq. (A6). Due to observation (A7) one can write the useful identities

$$\Xi_{nm}^{RR}(-iz + \omega_\nu, -iz) = \Xi_{mn}^{RR}(-iz, -iz + \omega_\nu)$$

$$\Xi_{nm}^{AA}(-iz, -iz - \omega_\nu) = \Xi_{mn}^{AA}(-iz - \omega_\nu, -iz)$$

$$\Xi_{nm}^{RA}(-iz + \omega_\nu, -iz) = \Xi_{mn}^{RA}(-iz, -iz + \omega_\nu)$$

and get for the contour integral in Eq. (A9) :

$$4\pi i I_{nm}^{AL}(\omega_\nu) = \int_{-\infty}^{\infty} \coth\left(\frac{z}{2T}\right) dz \left\{ [\Xi_{nm}^{RR}(-iz + \omega_\nu, -iz)]^2 L_m^R(-iz) - [\Xi_{nm}^{RA}(-iz + \omega_\nu, -iz)]^2 L_m^A(-iz) \right\} L_n^R(-iz + \omega_\nu) + \int_{-\infty - i\omega_\nu}^{\infty - i\omega_\nu} \coth\left(\frac{z}{2T}\right) dz \left\{ [\Xi_{nm}^{RA}(-iz + \omega_\nu, -iz)]^2 L_n^R(-iz + \omega_\nu) - [\Xi_{nm}^{AA}(-iz + \omega_\nu, -iz)]^2 L_n^A(-iz + \omega_\nu) \right\} L_m^A(-iz).$$

The last integration can be reduced to that along the real axis by means of shifting the variable $-iz + \omega_\nu \rightarrow -iz'$. The resulting expression (A9) for the electromagnetic response operator – still defined on Matsubara frequencies ω_ν – takes the form:

$$Q_{xx}^{AL}(\omega_\nu) = 4ie^2\nu_0^2\mathcal{D}^2\frac{eH}{\pi}\sum_{n,m}C_{mn}\int_{-\infty}^{\infty}\coth\left(\frac{z}{2T}\right)\Phi_{mn}(z,\omega_\nu)dz, \quad (\text{A11})$$

where

$$\Phi_{mn}(z,\omega_\nu) = \left\{ [\Xi_{nm}^{RR}(-iz + \omega_\nu, -iz)]^2 L_m^R(-iz) - [\Xi_{nm}^{RA}(-iz + \omega_\nu, -iz)]^2 L_m^A(-iz) \right\} L_n^R(-iz + \omega_\nu) + \left\{ [\Xi_{mn}^{RA}(-iz - \omega_\nu, -iz)]^2 L_n^R(-iz) - [\Xi_{nm}^{AA}(-iz, -iz - \omega_\nu)]^2 L_n^A(-iz) \right\} L_m^A(-iz - \omega_\nu). \quad (\text{A12})$$

The rules for performing the analytical continuations of the function $\Xi_{mn}(\Omega_k, \Omega_k + \omega_\nu)$ in Eq. (A12) are simple: the sign of the explicitly written absolute values of the corresponding frequency in Eq. (A6) is chosen as “+” in the case of retarded continuation (superscript R) and it is chosen as “-” in the case of the advanced one (superscript A). For instance

$$\Xi_{mn}^{RA}(\Omega_k, \Omega_k + \omega_\nu) = \frac{1}{2\omega_c(n-m)} \left[\psi\left(\frac{1}{2} + \frac{\omega_\nu - \Omega_k + \omega_c(n+1/2)}{4\pi T}\right) - \psi\left(\frac{1}{2} + \frac{-\Omega_k + \omega_c(m+1/2)}{4\pi T}\right) + \psi\left(\frac{1}{2} + \frac{\omega_\nu + \Omega_k + \omega_c(n+1/2)}{4\pi T}\right) - \psi\left(\frac{1}{2} + \frac{2\omega_\nu + \Omega_k + \omega_c(m+1/2)}{4\pi T}\right) \right]$$

and analogously for Ξ_{nm}^{RR} and Ξ_{nm}^{AA} .

Now one can perform the last analytical continuation $\omega_\nu \rightarrow -i\omega$ in Eq. (A12) and obtain $\Phi_{mn}^{(R)}(z, \omega)$ as an analytic function of the real external frequency ω . Since we are interested in the d.c. limit of the FC, i.e. $\omega \rightarrow 0$, the function $\Phi_{mn}^{(R)}(z, \omega)$ can be presented in the form of its Taylor expansion:

$$\Phi_{mn}^{(R)}(z, \omega) = \Phi_{mn}^{(R)}(z, 0) - \frac{i\omega}{\omega_c^2(n-m)^2} F_{nm}(-iz).$$

The first term is not of interest here: all frequency independent contributions which form $Q^{(\text{fl})}(0, T, H)$ are cancelled out: this is a necessary requirement of the absence of the diamagnetic response in the normal phase of superconductors. Actually, in order to find the FC we need to know only $\text{Im}Q^{(\text{fl})}(\omega, T, H)$, i.e. we are interested only

the imaginary part of $F_{nm}(-iz)$. It can be obtained by expansion of all functions $\Xi_{nm}^{\alpha\beta}$ ($\alpha, \beta = R, A$) and propagators in $\Phi_{mn}^{(R)}(z, \omega)$ over ω . Introducing the function

$$\Psi_{nm}(iz) = \psi\left(\frac{1}{2} + \frac{iz + \omega_c(n+1/2)}{4\pi T}\right) - \psi\left(\frac{1}{2} + \frac{iz + \omega_c(m+1/2)}{4\pi T}\right)$$

one can find the analytically continued expressions for the products of Eq. (A12):

$$\begin{aligned} [\Xi_{nm}^{RR}]^2 &= \frac{[\Psi_{nm}^2(-iz) - \frac{i\omega}{2\pi T} \Psi_{nm}(-iz) \Psi'_{nm}(-iz)]}{\omega_c^2 (n-m)^2}, \\ [\Xi_{mn}^{RA}(-iz \pm i\omega, -iz)]^2 &= \frac{\text{Re} \Psi_{nm}(-iz)}{\omega_c^2 (n-m)^2} \left[\text{Re} \Psi_{nm}(-iz) \pm \frac{i\omega}{4\pi T} \Psi'_{nm}(\pm iz) \right], \\ [\Xi_{nm}^{AA}]^2 &= \frac{1}{\omega_c^2 (n-m)^2} [\Psi_{nm}^2(iz) + O(\omega^2)] \end{aligned}$$

which leads to

$$\begin{aligned} \text{Im} F_{nm}(-iz) &= -\frac{\partial}{\partial z} \left\{ 2\text{Re} \Psi_{nm}^2 \text{Im} L_m^R \text{Im} L_n^R \right. \\ &\quad \left. + \text{Im} \Psi_{nm}^2 [\text{Im} L_n^R \text{Re} L_m^R + \text{Im} L_m^R \text{Re} L_n^R] \right\}. \end{aligned}$$

One can see that this function is symmetric with respect to subscripts permutation: $\text{Im} F_{nm}(-iz) = \text{Im} F_{mn}(-iz)$. Let us stress that we have could present the linear in ω part of the function $\Phi_{mn}^{(R)}(z, \omega)$ in the form of full derivative with respect to z . The same situation was found in the original paper of Aslamazov and Larkin² for the simple case when the Green functions block could

be assumed to be constant. As a consequence of this important property of $\Phi_{mn}^{(R)}(z, \omega)$, the integration over z in Eq. (A11) can be performed by parts. After summation over m , the Eqs. (1) and (A8) read as

$$\begin{aligned} \delta\sigma_{xx}^{\text{AL}}(T, H) &= \frac{e^2}{2\pi T} \nu_0^2 \sum_{n=0}^{\infty} (n+1) \int_{-\infty}^{\infty} \frac{dz}{\sinh^2(z/2T)} \\ &\times \left\{ 2\text{Re} \Psi_{n,n+1}^2(-iz) \text{Im} L_n^R(-iz) \text{Im} L_{n+1}^R(-iz) \right. \\ &\quad \left. + \text{Im} \Psi_{n,n+1}^2(-iz) [\text{Im} L_n^R(-iz) \text{Re} L_{n+1}^R(-iz) \right. \\ &\quad \left. + \text{Im} L_{n+1}^R(-iz) \text{Re} L_n^R(-iz)] \right\}. \end{aligned} \quad (\text{A13})$$

Let us attract the attention to the fact that due to the integration by parts $\coth z/2T$ disappeared from the integral Eq. (A11) being replaced in Eq. (A13) by its derivative $\sinh^{-2}(z/2T)$. This fact makes our answer different from the one of Ref. [15] and physically means, as we will see below, that at low temperatures the paraconducting contribution tend to zero: fluctuation Cooper pairs above $H_{c2}(0)$ exist but do not move and do not participate directly in the charge transfer^{1,11}.

It is convenient to introduce the dimensionless variable: $x = z/(2\pi T)$, parameters $t = T/T_{c0}$ and $h = 2e\xi^2 H$, where $\xi^2 = \pi D/(8T)$, and the function

$$\mathcal{E}_m(t, h, ix) = \ln t + \psi \left[\frac{1+ix}{2} + \frac{2}{\pi^2} \left(\frac{h}{t} \right) (2m+1) \right] - \psi \left(\frac{1}{2} \right). \quad (\text{A14})$$

In this representation, Eq. (A13) takes the form ($\mathcal{E}_k(t, h, ix) \equiv \mathcal{E}_k$)

$$\delta\sigma_{xx}^{\text{AL}}(t, h) = \frac{e^2}{\pi} \sum_{m=0}^{\infty} (m+1) \int_{-\infty}^{\infty} \frac{dx}{\sinh^2 \pi x} \left\{ \frac{\text{Im}^2 \mathcal{E}_m}{|\mathcal{E}_m|^2} + \frac{\text{Im}^2 \mathcal{E}_{m+1}}{|\mathcal{E}_{m+1}|^2} + \frac{\text{Im}^2 \mathcal{E}_{m+1} - \text{Im}^2 \mathcal{E}_m}{|\mathcal{E}_m|^2 |\mathcal{E}_{m+1}|^2} \text{Re} [\mathcal{E}_m \mathcal{E}_{m+1}] \right\}. \quad (\text{A15})$$

This is the general expression for fluctuation paraconductivity valid in all domains of temperatures and fields under consideration.

We will see that all diagrams presented in Fig.1 are relevant in different regions of the phase diagram, depicted in Fig. 5. Nine regions of different asymptotic behavior can be distinguished and below we will analyze all contributions in each domain.

2. Asymptotic behavior

a. Vicinity of T_{c0} , fields $h \ll 1(H \ll H_{c2}(0))$

In this case $\ln t = \epsilon \ll 1$ and the ψ -function in Eq.(A14) can be expanded. In first approximation:

$$\mathcal{E}_m^{(1)}(t, h, ix) = \epsilon + \frac{i\pi^2 x}{4} + \left(\frac{2h}{t} \right) \left(m + \frac{1}{2} \right). \quad (\text{A16})$$

The integral in Eq. (A15) can be easily carried out: only the first fraction in the parenthesis should be taken into account. Further summation over Landau levels can be performed exactly in terms of the ψ -function:

$$\delta\sigma_{xx}^{\text{AL}}(\epsilon, h \ll 1) = \frac{e^2}{2\epsilon} \left(\frac{\epsilon}{2h} \right)^2 \left[\psi \left(\frac{1}{2} + \frac{\epsilon}{2h} \right) - \psi \left(\frac{\epsilon}{2h} \right) - \frac{h}{\epsilon} \right], \quad (\text{A17})$$

which coincides with the known expression for the Cooper pairs contribution to the magneto-conductivity in the Ginzburg-Landau region¹.

The general Eq. (A15) allows to obtain the next order correction in ϵ with respect to the AL result. In order to do this, one should take into account both terms and expand up to the second order:

$$\begin{aligned} \mathcal{E}_m^{(2)}(t, h, ix) &= \mathcal{E}_m^{(1)}(t, h, ix) - \frac{14\zeta(3)ix}{\pi^2} \left(\frac{2h}{t} \right) \left(m + \frac{1}{2} \right) \\ &\quad + 7\zeta(3) \frac{x^2}{4} - \frac{28\zeta(3)}{\pi^4} \left(\frac{2h}{t} \right)^2 \left(m + \frac{1}{2} \right)^2 \end{aligned} \quad (\text{A18})$$

After some simple but cumbersome calculation in the limit of small fields, one finds

$$\delta\sigma_{xx}^{\text{AL}}(\epsilon \ll 1) = \frac{e^2}{16\epsilon} - \frac{7\zeta(3)e^2}{8\pi^4} \ln \frac{1}{\epsilon}, \quad (\text{A19})$$

which demonstrates that the next order correction to the well known AL result in the vicinity of T_{c0} is smaller than the DOS⁵ and the regular MT¹ contributions (see below) by only numerical pre-factor.

b. High temperatures $T \gg T_{c0}$, weak fields $h \ll t$

Let us move to the discussion of the high-temperature asymptotic. We will assume $\ln t \gg 1$ in Eq. (A14) and get:

$$\text{Im}\mathcal{E}_m(t, h, ix) = \frac{x}{2} \psi' \left[\frac{1}{2} + \frac{4}{\pi^2} \left(\frac{h}{t} \right) (m + 1/2) \right]. \quad (\text{A20})$$

The sum in Eq. (A15) converges at $n_{\text{max}} \sim t/h \gg 1$ and can be replaced by an integral. The integration over x involves only the region $x \sim 1$ and can be performed first. As a result one gets

$$\delta\sigma_{xx}^{\text{AL}}(t \gg 1, h \ll t) = \frac{e^2}{6\pi^2} \frac{C_1}{\ln^3 t}$$

with $C_1 = \frac{1}{3} \int_0^\infty [\psi'(1/2 + x)]^3 dx = 6.97$. Let us stress that this asymptotic expression coincides with the high temperature behavior of the AL contribution obtained in clean case¹⁹ which emphasises the statement that the 2D paraconductivity is an universal function of $\ln t$ throughout the complete temperature range.

c. Fields close to the line $H_{c2}(T)$

The line separating normal and superconducting phases $H_{c2}(T)$ (in our dimensionless units the line of critical fields $h_{c2}(t)$) is determined by the requirement that the propagator (2) has a pole when $\Omega_k = 0$ and $m = 0$:

$$\ln t + \psi \left(\frac{1}{2} + \frac{2}{\pi^2} \frac{h_{c2}(t)}{t} \right) - \psi \left(\frac{1}{2} \right) = 0.$$

At low temperatures $T \ll T_{c0}$, close to the point $T = 0$ and $H = H_{c2}(0)$, the critical field is $h_{c2}(t) = 2\xi^2 H_{c2}(0)/e \sim 1$. Then one can substitute the ψ -function by its asymptotic expression $\psi(x) = \ln x - 1/(2x)$ and take into account that $\psi(1/2) = -\ln 4\gamma_E$ ($\gamma_E = 1.781..$ is the Euler's constant) which results in

$$h_{c2}(t \rightarrow 0) = \frac{\pi^2}{8\gamma_E}. \quad (\text{A21})$$

In order to find the paraconducting contribution to FC above the curve $H_{c2}(T)$ in Fig. 5, let us rewrite Eq.

(A14) in terms of the reduced field

$$\tilde{h}(t) = \frac{h - h_{c2}(t)}{h_{c2}(t)} \ll 1$$

Below we will see that the Cooper pair contribution to FC, which is singular in \tilde{h}^{-1} , originates in Eq. (A15) only from the term with $m = 0$, i.e. we can restrict ourselves to the Lowest Landau Level (LLL) approximation. Hence we will need the explicit expression for $\mathcal{E}_m(t, \tilde{h}, ix)$ only for $m = 0, 1$ and $\tilde{h} \ll t \ll h_{c2}(t)$. In order to get this, one can use in Eq. (A14) a parametrization in terms of \tilde{h} and expand it $\tilde{h} \ll 1$ and $h - h_{c2}(t) = \tilde{h} \cdot h_{c2}(t) \ll t$. This gives

$$\mathcal{E}_0(t, \tilde{h}, ix) = \tilde{h} + \frac{i\pi^2 xt}{4h_{c2}(t)}. \quad (\text{A22})$$

The substitution of Eq. (A22) to Eq. (A15) results in

$$\delta\sigma_{xx}^{\text{AL}}(t, h) = \frac{e^2}{\pi^2} J_{GL} \left(\frac{4h_{c2}(t)\tilde{h}}{\pi^2 t} \right). \quad (\text{A23})$$

with

$$J_{GL}(r) = \int_{-\infty}^{\infty} \frac{dx}{\sinh^2 x} \frac{x^2}{x^2 + \pi^2 r^2} = 2r\psi'(r) - \frac{1}{r} - 2 \quad (\text{A24})$$

first calculated in Ref. [15]. This formula is valid along all the line $h_{c2}(t)$ until $t \sim h_{c2}(t)$. Taking into account the asymptotic expressions

$$\psi'(r \rightarrow \infty) = \frac{1}{r} + \frac{1}{2r^2} + \frac{1}{6r^3}; \quad \psi'(r \rightarrow 0) = 1/r^2. \quad (\text{A25})$$

one finds that in this domain

$$\delta\sigma_{xx}^{\text{AL}}(t, h) = \begin{cases} \frac{4e^2\gamma_E^2 t^2}{3\pi^2 h^2}, & t \ll \tilde{h}, \\ \frac{e^2 t}{4h_{c2}(t)h}, & h_{c2}(t)\tilde{h} \ll t. \end{cases} \quad (\text{A26})$$

The first line of Eq. (A26) corresponds to the *quantum fluctuations* which are realized in the limit of lowest temperatures $t \ll \tilde{h}$ close to $H_{c2}(0)$. One sees that the paraconductivity decays here as T^2 . In the temperature range $h_{c2}(t)\tilde{h} \ll t \ll h_{c2}(t)$ the paraconductivity is determined by the first line of Eq. (A26). Close to $H_{c2}(0)$ but for relatively high temperatures $t \sim \tilde{h}$ the corresponding expression can be rewritten using the explicit expression for $h_{c2}(0)$ Eq. (A21):

$$\delta\sigma_{xx}^{\text{AL}}(t, h) = \frac{2\gamma_E e^2}{\pi^2} \left(\frac{t}{\tilde{h}} \right), \quad (\text{A27})$$

which perfectly matches to the first line of the Eq. (A26). Here the transition from quantum to classical fluctuations takes place. At higher temperatures along the line $h_{c2}(t)$ one should take into account the temperature dependence of $h_{c2}(t)$:

$$\delta\sigma_{xx}^{\text{AL}}(t, h) = \frac{e^2}{4} \frac{t}{h - h_{c2}(t)}. \quad (\text{A28})$$

This expression is valid along the line $h_{c2}(t)$ until $t \ll h_{c2}(t)$ where Eq. (A28) matches to Eq. (A17).

d. High fields ($H \gg H_{c2}(0)$), temperatures $t \ll h$

In this domain we are far from the transition line $H_{c2}(T)$, [$h \gg h_{c2}(t)$] and the LLL approximation is not applicable. Nevertheless, one can substitute the summation over Landau levels by an integration. Replacing the ψ -function in Eq. (A14) by a logarithm, one finds that

$$\mathcal{E}_m(t, h, ix) = \ln \frac{4h}{\pi^2} \left(m + \frac{1}{2} \right) - \psi \left(\frac{1}{2} \right) + \frac{i\pi^2 xt}{4h(2m+1)}. \quad (\text{A29})$$

One can see that this expression reproduces Eq. (A22) when $h \rightarrow h_{c2}(t)$ and $m = 0$. Let us substitute Eq. (A29) to Eq. (A15). As we will see below, the sum converges at $m \sim 1$. It is why the main contribution comes from the second term of Eq. (A15), where the sum $\text{Im}\mathcal{E}_m \text{Re}\mathcal{E}_{m+1} + \text{Im}\mathcal{E}_{m+1} \text{Re}\mathcal{E}_m \sim \ln \left(\frac{4h}{\pi^2} \right)$. As a result we get

$$\delta\sigma_{xx}^{\text{AL}}(t, h) = \frac{\pi^2 e^2}{192} \left(\frac{t}{h} \right)^2 \frac{C_2}{\ln^3 \frac{2h}{\pi^2}}$$

with $C_2 = 0.545$. Let us recall that this expression is valid for arbitrary temperatures small in comparison to reduced field $t \ll h$.

Appendix B: Maki-Thompson contribution

1. General expression

Below we will calculate the fluctuation renormalization of the one-electron contributions to conductivity. It is technically convenient to start with the usual expressions for the Maki-Thompson and other diagrams from Fig. 1, written in momentum representation. Only at the very end one should quantize the motion of Cooper pairs in a magnetic field in accordance with the rule

$$\frac{\mathcal{D}}{8T} \int \frac{d^2q}{(2\pi)^2} f[\mathcal{D}q^2] = \frac{h}{2\pi^2 t} \sum_{m=0}^M f[\omega_c(n+1/2)].$$

Diagram 2 from Fig. 1 can be written as

$$Q_{xx}^{\text{MT}}(\omega_\nu) = 2e^2 T \sum_{\Omega_k} \int \frac{d^2\mathbf{q}}{(2\pi)^2} L(\mathbf{q}, \Omega_k) \Sigma_{xx}^{\text{MT}}(\mathbf{q}, \Omega_k, \omega_\nu), \quad (\text{B1})$$

where

$$\begin{aligned} \Sigma_{xx}^{\text{MT}}(\mathbf{q}, \Omega_k, \omega_\nu) &= T \sum_{\varepsilon_n} \lambda(\mathbf{q}, \varepsilon_{n+\nu}, \Omega_{k-n-\nu}) \\ &\times \lambda(\mathbf{q}, \varepsilon_n, \Omega_{k-n}) I_{xx}^{\text{MT}}(\mathbf{q}, \varepsilon_n, \Omega_k, \omega_\nu) \end{aligned} \quad (\text{B2})$$

and

$$\begin{aligned} I_{xx}^{\text{MT}} &= \int \frac{d^3\mathbf{p}}{(2\pi)^3} v_x(\mathbf{p}) v_x(\mathbf{q}-\mathbf{p}) G(\mathbf{p}, \varepsilon_{n+\nu}) \\ &\times G(\mathbf{p}, \varepsilon_n) G(\mathbf{q}-\mathbf{p}, \Omega_{k-n-\nu}) G(\mathbf{q}-\mathbf{p}, \Omega_{k-n}). \end{aligned}$$

The main q -dependence in (B1) arises from the propagator and vertices λ . That is why we can assume $q = 0$ in the Green functions and calculate the electron momentum integral by changing, as usual, to a $\xi(\mathbf{p})$ integration:

$$\begin{aligned} I_{xx}^{\text{MT}} &= -\mathcal{D}\tau^{-1} \nu_0 \int_{-\infty}^{\infty} \frac{d\xi}{\xi - i\tilde{\varepsilon}_n} \frac{1}{\xi - i\tilde{\varepsilon}_{n+\nu}} \\ &\times \frac{1}{\xi - i\tilde{\Omega}_{k-n}} \frac{1}{\xi - i\tilde{\Omega}_{k-n-\nu}}. \end{aligned} \quad (\text{B3})$$

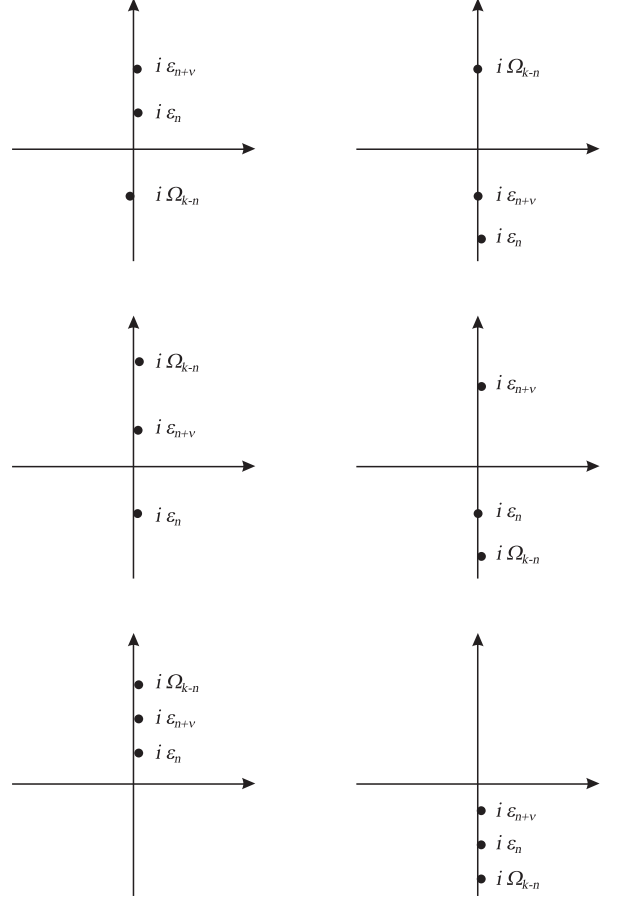


FIG. 12. ξ -integration in Eq. (B3): all six possible positions of the poles in the complex plane of ξ are shown.

This integral, Eq. (B3), can be calculated using the Cauchy theorem. Closing the contour in upper or lower half-plane by the large semicircle and noticing, that, due to fast decrease of the integrand the function in Eq. (B3), the integral over the semicircle becomes zero, one can express J_{xx} in terms of the sum of the corresponding residues. There are six different combinations of the pole positions with respect to the real axis in the complex plane of ξ , leading to non-zero results (see Fig. 12): two realization corresponding to $\theta(-\varepsilon_n \varepsilon_{n+\nu}) \theta(\Omega_{k-n} \Omega_{k-n-\nu}) \neq 0$, one realization corresponding to $\theta(-\varepsilon_n \varepsilon_{n+\nu}) \theta(-\Omega_{k-n} \Omega_{k-n-\nu}) \neq 0$, two realization corresponding to $\theta(\varepsilon_n \varepsilon_{n+\nu}) \theta(\Omega_{k-n} \Omega_{k-n-\nu}) \neq 0$.

0, and the realization corresponding to $\theta(\varepsilon_n \varepsilon_{n+\nu}) \theta(-\Omega_{k-n} \Omega_{k-n-\nu}) \neq 0$. Calculating the residues for each situation and assuming that $\tilde{\varepsilon}_n = (2\tau)^{-1} \text{sgn} \varepsilon_n$ (let us recall that we consider the disordered limit $T \ll \tau^{-1}$) one finds:

$$\begin{aligned} I_{xx}^{\text{MT}} &= 2\pi \mathcal{D} \nu_0 \tau^2 \{ \theta(-\varepsilon_n \varepsilon_{n+\nu}) \theta(\Omega_{k-n} \Omega_{k-n-\nu}) \\ &\quad + \theta(\varepsilon_n \varepsilon_{n+\nu}) \theta(-\Omega_{k-n} \Omega_{k-n-\nu}) \\ &\quad - 2\theta(-\varepsilon_n \varepsilon_{n+\nu}) \theta(-\Omega_{k-n} \Omega_{k-n-\nu}) \\ &\quad - 2\theta(\varepsilon_n \varepsilon_{n+\nu}) \theta(\Omega_{k-n} \Omega_{k-n-\nu}) \}. \end{aligned}$$

Now one should substitute this expression to Eq. (B2) and perform the summation over the fermionic frequencies. This is a cumbersome exercise, which, nevertheless, can be followed through analytically. Here we mention some useful transformations which are important to perform the summations: One can see, that the simultaneous permutations $n \rightarrow -n$ and $k \rightarrow -k$ allows to simplify the sums:

$$\begin{aligned} \Sigma_{xx}^{\text{MT}} &= \left(\Sigma_{xx}^{\text{MT}(an)} + \Sigma_{xx}^{\text{MT}(reg2)} \right) + \Sigma_{xx}^{\text{MT}(reg1)} = -2\pi \nu_0 \mathcal{D} T \\ &\times \left\{ \sum_{n=-\nu}^{-1} \frac{2\theta(-\Omega_{k-n} \Omega_{k-n-\nu}) - \theta(\Omega_{k-n} \Omega_{k-n-\nu})}{(|\varepsilon_{n+\nu} - \Omega_{k-n-\nu}| + \mathcal{D}q^2)(|\varepsilon_n - \Omega_{k-n}| + \mathcal{D}q^2)} \right. \\ &\quad \left. + 2 \sum_{n=0}^{\infty} \frac{2\theta(\Omega_{k-n} \Omega_{k-n-\nu}) - \theta(-\Omega_{k-n} \Omega_{k-n-\nu})}{(|\varepsilon_{n+\nu} - \Omega_{k-n-\nu}| + \mathcal{D}q^2)(|\varepsilon_n - \Omega_{k-n}| + \mathcal{D}q^2)} \right\}. \end{aligned}$$

The rules writing the absolute values explicitly in the sum using the first θ -function is evident. In the second sum, containing $\theta(\Omega_{k-n} \Omega_{k-n-\nu})$, one should make a shift $n' = n + \nu$. After rewriting the absolute values for the Cooperons, the sums can be expressed in terms of ψ -functions. Using the identity

$$\psi(1/2 + iz) - \psi(1/2 - iz) = \pi i \tanh \pi z$$

allows to write the final expression for the first sum as

$$\begin{aligned} \Sigma_{xx}^{\text{MT}(an)} + \Sigma_{xx}^{\text{MT}(reg2)} &= -\frac{\mathcal{D} \nu_0 \theta(\omega_{\nu-1} - |\Omega_k|)}{2(\omega_\nu + \mathcal{D}q^2)} \\ &\left[\psi\left(\frac{1}{2} + \frac{2\omega_\nu - |\Omega_k| + \mathcal{D}q^2}{4\pi T}\right) - \psi\left(\frac{1}{2} + \frac{|\Omega_k| + \mathcal{D}q^2}{4\pi T}\right) \right]. \end{aligned} \quad (\text{B4})$$

Looking at the denominator of this expression one can recognize that $\Sigma_{xx}^{\text{MT}(an)}$ is responsible for the anomalous Maki-Thompson term.

Next we consider the remaining second sum in Σ_{xx}^{MT} . One can see that in the first term both arguments of the absolute values are positive. In the second term we can replace $k \rightarrow -k$, with an additional change of the order of the summation over bosonic frequencies. The sum with $\theta(\Omega_{k-n} \Omega_{k-n-\nu})$ can be calculated in the spirit of Eq. (B4). Regarding the last sum, containing $\theta(-\Omega_{k-n} \Omega_{k-n-\nu})$, one can find that it is exactly equals

to zero for any Ω_k . Finally

$$\begin{aligned} \Sigma_{xx}^{\text{MT}(reg1)} &= -\frac{\mathcal{D} \nu_0}{\omega_\nu} \left[\psi\left(\frac{1}{2} + \frac{2\omega_\nu + |\Omega_k| + \mathcal{D}q^2}{4\pi T}\right) \right. \\ &\quad \left. - \psi\left(\frac{1}{2} + \frac{|\Omega_k| + \mathcal{D}q^2}{4\pi T}\right) \right]. \end{aligned} \quad (\text{B5})$$

Using the explicit Eqs. (B4)-(B5) we can perform the final summation over bosonic frequencies in Eq. (B1) and the analytical continuation of $Q_{xx}^{\text{MT}}(\omega_\nu)$ to the axis of real frequencies. The analytical continuation of $Q_{xx}^{\text{MT}(reg1)}$ is trivial since Eq. (B5) is the analytical function of ω_ν . As a result we get

$$\begin{aligned} Q_{xx}^{\text{MT}(reg1)\text{R}}(\omega) &= i\omega e^2 \frac{\mathcal{D} \nu_0}{4\pi^2 T} \int \frac{d^2 \mathbf{q}}{(2\pi)^2} \\ &\quad \times \sum_{k=-\infty}^{\infty} L(\mathbf{q}, \Omega_k) \psi''\left(\frac{1}{2} + \frac{|\Omega_k| + \mathcal{D}q^2}{4\pi T}\right). \end{aligned}$$

Next we go over from the integration over the momentum of the Cooper pair center of mass \mathbf{q} to the summation over Landau levels. Recalling that the density of states at the Landau level is H/Φ_0 , one finds

$$\delta\sigma_{xx}^{\text{MT}(reg1)} = \frac{e^2}{4\pi^2 T} \frac{\mathcal{D}H}{\Phi_0} \sum_m \sum_{k=-\infty}^{\infty} \frac{4\mathcal{E}_m''(t, h, |k|)}{\mathcal{E}_m(t, h, |k|)}, \quad (\text{B6})$$

where $\mathcal{E}_m^{(p)}(t, h, z) \equiv \partial_z^p \mathcal{E}_m(t, h, z)$, i.e

$$\mathcal{E}_m''(t, h, |k|) = \psi''\left[\frac{1 + |k|}{2} + \frac{2h}{\pi^2 t}(2m + 1)\right].$$

In the part of the electromagnetic operator related to Eq. (B4), the external frequency ω_ν appears in the upper limit of the bosonic sum:

$$\begin{aligned} &Q_{xx}^{\text{MT}(an)} + Q_{xx}^{\text{MT}(reg2)} \\ &= -2e^2 T \mathcal{D} \nu_0 \int \frac{d^2 \mathbf{q}}{(2\pi)^2} \frac{1}{\omega_\nu + \mathcal{D}q^2} \sum_{|k|=0}^{\nu-1} L(\mathbf{q}, \Omega_k) \\ &\left[\psi\left(\frac{1}{2} + \frac{2\omega_\nu - |\Omega_k| + \mathcal{D}q^2}{4\pi T}\right) - \psi\left(\frac{1}{2} + \frac{|\Omega_k| + \mathcal{D}q^2}{4\pi T}\right) \right] \end{aligned}$$

and the procedure of analytical continuation is more sophisticated. First of all one can easily see that the contributions of positive and negative k are equal. The method to continue such a sum the real frequencies was developed in Ref. [7] and consists in an Eliashberg transformation of the sum over Ω_k to an integral over the contour \mathcal{C} (see Fig. 13 and the detailed description of this procedure in Ref. [1]). One finds

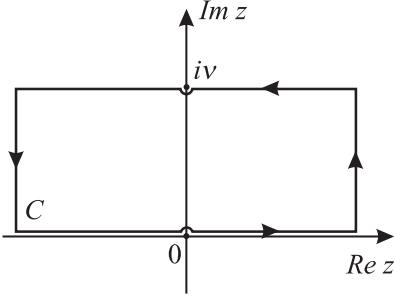


FIG. 13. Integration contour used in the analytic continuation of the MT contribution.

$$\begin{aligned}
Q_{xx}^{\text{MT(an)}} + Q_{xx}^{\text{MT(reg2)R}} &= -4e^2 T \mathcal{D} \nu_0 \int \frac{d^2 \mathbf{q}}{(2\pi)^2} \frac{1}{\omega_\nu + \mathcal{D}q^2} \\
&\left\{ \frac{1}{2} L(\mathbf{q}, 0) \left[\psi \left(\frac{1}{2} + \frac{2\omega_\nu + \mathcal{D}q^2}{4\pi T} \right) - \psi \left(\frac{1}{2} + \frac{\mathcal{D}q^2}{4\pi T} \right) \right] \right. \\
&+ \frac{1}{2i} \oint_{C_2} dz \coth(\pi z) L(\mathbf{q}, -iz) \left[\psi \left(\frac{1}{2} + \frac{2\omega_\nu + \mathcal{D}q^2}{4\pi T} + \frac{iz}{2} \right) \right. \\
&\left. \left. - \psi \left(\frac{1}{2} + \frac{iz}{2} + \frac{\mathcal{D}q^2}{4\pi T} \right) \right] \right\}.
\end{aligned}$$

The residue at the point $z = i\nu$ is equal to zero. Shifting the variables in the integral over the upper line $\text{Im}z = \nu$ as $z_1 = z' + i\nu$, one can present Q_{xx}^{MT} as an analytical function of ω_ν and analytically continue it in the standard way $i\omega_\nu \rightarrow \omega \rightarrow 0$. Expanding it in small ω and integrating by parts, one gets

$$\begin{aligned}
\delta\sigma_{xx}^{\text{MT(an)}} + \delta\sigma_{xx}^{\text{MT(reg2)}} &= \\
&= \frac{e^2}{2} \mathcal{D} \int \frac{d^2 \mathbf{q}}{(2\pi)^2} \frac{1}{\tau_\phi^{-1} + \mathcal{D}q^2} \int_{-\infty}^{\infty} \frac{dz}{\sinh^2 \pi z} \frac{\psi \left(\frac{1-iz}{2} + \frac{\mathcal{D}q^2}{4\pi T} \right) - \psi \left(\frac{1+iz}{2} + \frac{\mathcal{D}q^2}{4\pi T} \right)}{\ln \frac{T}{T_c} + \psi \left(\frac{1-iz}{2} + \frac{\mathcal{D}q^2}{4\pi T} \right) - \psi \left(\frac{1}{2} \right)}
\end{aligned}$$

This expression is then transformed to the summations over Landau levels and written in the dimensionless variables, in the same way as it was done before. Adding the regular part Eq. (B6), we finally write the most general expression for the MT contribution valid in all domains of temperatures and magnetic field under consideration:

$$\begin{aligned}
\delta\sigma^{\text{MT}} &= \delta\sigma_{xx}^{\text{MT(reg1)}} + \left(\delta\sigma_{xx}^{\text{MT(an)}} + \delta\sigma_{xx}^{\text{MT(reg2)}} \right) \\
&= \frac{e^2}{\pi^4} \left(\frac{h}{t} \right) \sum_{m=0}^M \left\{ \sum_{k=-\infty}^{\infty} \frac{4\mathcal{E}_m''(t, h, |k|)}{\mathcal{E}_m(t, h, |k|)} + \frac{\pi^3}{\gamma_\phi + \frac{2h}{t}(m+1/2)} \int_{-\infty}^{\infty} \frac{dz}{\sinh^2 \pi z} \frac{\text{Im}^2 \mathcal{E}_m(t, h, iz)}{\text{Re}^2 \mathcal{E}_m(t, h, iz) + \text{Im}^2 \mathcal{E}_m(t, h, iz)} \right\}.
\end{aligned} \tag{B7}$$

where $M = (tT_{c0}\tau)^{-1}$ is the cut-off parameter.

2. Asymptotic behavior

a. Contribution $\delta\sigma_{xx}^{\text{MT(reg1)}}$

Let us start with the evaluation of the contribution $\delta\sigma_{xx}^{\text{MT(reg1)}}$ given by Eq. (B6).

Vicinity of T_{c0} , fields $h \ll 1(H \ll H_{c2}(0))$. — Here one can just use Eq. (A14) for integer argument k , considering the smallness of h/t , expand the ψ -function, and perform the summation exactly:

$$\delta\sigma_{xx}^{\text{MT(reg1)}}(\epsilon \ll 1, h) = -\frac{7\zeta(3)e^2}{\pi^4} \left[\psi \left(\frac{t}{2h} \right) - \psi \left(\frac{1}{2} + \frac{\epsilon t}{2h} \right) \right]. \tag{B8}$$

High temperatures $T \gg T_{c0}$, weak fields $h \ll t$. — For the high-temperature asymptotic of Eq. (B6), we assume $\ln t \gg 1$. The sum over k is determined by $\mathcal{E}_m''(t, h, |k|)$ and converges fast: it can be performed in first. The remaining sum over Landau levels slowly diverges at large m_{max} and can be substituted by an integral. The double logarithmic divergence of this integral at the upper limit should be cut off at the limit corresponding $m_{\text{max}} \sim (T_{c0}\tau)^{-1}$ which results in

$$\delta\sigma_{xx}^{\text{MT(reg1)}} = -\frac{e^2}{\pi^2} \left[\ln \ln \frac{1}{T_{c0}\tau} - \ln \ln t \right]. \tag{B9}$$

One can see that close to T_{c0} $\ln(\ln \ln t) \rightarrow \ln(\frac{1}{\epsilon})$, Eqs. (B9) and (B8) therefore match each other.

Fields close to the line $H_{c2}(T)$. — In this domain, as above, one can use the LLL approximation. Nevertheless, since $t \ll h_{c2}(t)$, many terms are involved in the sum over k in Eq. (B6). Therefore it is convenient to present the function $\mathcal{E}_0(t, \tilde{h}, |k|)$ in this case in the form

$$\mathcal{E}_0(t, \tilde{h}, |k|) = \psi \left[\frac{1+|k|}{2} + \frac{2}{\pi^2} \frac{h_{c2}(t)}{t} (1 + \tilde{h}(t)) \right] - \psi \left(\frac{1}{2} + \frac{2}{\pi^2} \frac{h_{c2}(t)}{t} \right)$$

and taking into account the asymptotic expression (A25) one finds

$$\delta\sigma_{xx}^{\text{MT}(\text{reg1})} = -\frac{e^2}{2} \frac{1}{\tilde{h}(t)} \left(\frac{t}{2h} \right) - \frac{2e^2}{\pi^2} \left[\ln \frac{2h}{\pi^2 t} - \psi \left(1 + \frac{4}{\pi^2} \frac{h_{c2}(t)}{t} \tilde{h}(t) \right) \right].$$

Along the line $H_{c2}(T)$, in the region of classic fluctuations $\tilde{h} \lesssim t \ll h_{c2}(t)$ Eq. (B6) contains two contributions: one, originating from the term with $k=0$, is singular in $h(t) - h_{c2}(t)$, the second is logarithmic in reduced temperature:

$$\delta\sigma_{xx}^{\text{MT}(\text{reg1})} = -\frac{e^2}{4} \frac{t}{h - h_{c2}(t)} - \frac{2e^2}{\pi^2} \ln \frac{2h_{c2}(t)}{\pi^2 t}. \quad (\text{B10})$$

In the regime of quantum fluctuations $t \lesssim \tilde{h}$, we get

$$\delta\sigma_{xx}^{\text{MT}(\text{reg1})} = -\frac{2\gamma_E e^2}{\pi^2} \frac{t}{\tilde{h}} - \frac{2e^2}{\pi^2} \ln \frac{1}{\tilde{h}}. \quad (\text{B11})$$

High fields $H \gg H_{c2}(0)$, temperatures $t \ll h$. — This domain is analogous to the previous one. As above,

$$\delta\sigma_{xx}^{\text{MT}} = \frac{e^2}{8} \frac{1}{\epsilon - \gamma_\phi} \left[\psi \left(1/2 + \frac{t\epsilon}{2h} \right) - \psi \left(1/2 + \frac{t\gamma_\phi}{2h} \right) \right] - \frac{14\zeta(3)e^2}{\pi^4} \left[\ln \left(\frac{t}{2h} \right) - \psi \left(1/2 + \frac{t\epsilon}{2h} \right) \right]. \quad (\text{B13})$$

This formula is valid in the vicinity of the critical temperature T_{c0} , where we have three different regimes [weak fields $h \ll \epsilon$, GL strong fields $\epsilon \ll h$, and fields close to the $h_{c2}(\epsilon)$ line which is "mirrored" at T_{c0}].

High temperatures $T \gg T_{c0}$, weak fields $h \ll t$. — Here we discuss the high-temperature asymptotic. As it was done before, we assume $\ln t \gg 1$ and use Eqs. (A14) and (A20). Integration over x due to the factor $\cosh^{-2} \pi z$ involves only the region $z \sim 1$ and can be performed first. The sum over Landau levels in this case converges at large $m_{\text{max}} \sim t/h \gg 1$ and it can be substituted by an integral. The contributing part of the integration with logarithmic

we first perform the summation over k and integrate over Landau levels:

$$\delta\sigma_{xx}^{\text{MT}(\text{reg1})} = -\frac{e^2}{\pi^2} \left(\ln \ln \frac{1}{T_{c0}\tau} - \ln \ln \frac{2h}{\pi^2} \right). \quad (\text{B12})$$

The only difference between Eqs. (B9) and (B12) consists in the lower limit: in the former it is determined by the temperature while in the latter its role is taken by the zero Landau level $\omega_c \gg T$. Eq. (B12) is valid for arbitrary temperatures smaller ω_c and it obviously matches Eq. (B11) along the axis of the magnetic field ($t=0$).

b. Contribution $\delta\sigma_{xx}^{\text{MT}(\text{an})} + \delta\sigma_{xx}^{\text{MT}(\text{reg2})}$

Now we consider the second part of the MT contribution Eq. (B7), namely $\delta\sigma_{xx}^{\text{MT}(\text{an})} + \delta\sigma_{xx}^{\text{MT}(\text{reg2})}$.

Vicinity of T_{c0} , fields $h \ll 1$ ($H \ll H_{c2}(0)$). — In the vicinity of the critical temperature T_{c0} one should use the expansion Eqs. (A16)-(A18) of $\mathcal{E}_m(t, h, ix)$. For the second order correction it is sufficient to take on only the imaginary part of $\mathcal{E}_m(t, h, ix)$ into account. Substituting correspondingly $\text{Re}\mathcal{E}_m^{(1)}(\epsilon, h \ll 1, ix)$ and $\text{Im}\mathcal{E}_m^{(2)}(\epsilon, h \ll 1, ix)$ to Eq. (B7) and using the fact that $\gamma_\phi \ll 1$, the integral over x can be easily performed [it converges for $x > x_0 \sim \epsilon + (\frac{h}{t})(2m+1)$]. The remaining summation is accomplished in terms of the ψ -functions and its result consists of two terms: the first one corresponds to the anomalous MT term $\delta\sigma_{xx}^{\text{MT}(\text{an})}$, while the second, $\delta\sigma_{xx}^{\text{MT}(\text{reg2})}$, exactly coincides in this region with $\delta\sigma_{xx}^{\text{MT}(\text{reg1})}$ [Eq. (B10)]. Therefore, we present the total $\delta\sigma_{xx}^{\text{MT}} = \delta\sigma_{xx}^{\text{MT}(\text{reg1})} + \delta\sigma_{xx}^{\text{MT}(\text{an})} + \delta\sigma_{xx}^{\text{MT}(\text{reg2})}$, which takes the form

accuracy turns out to be only the fraction containing γ_ϕ . As result we get:

$$\delta\sigma_{xx}^{\text{MT}(\text{an})} + \delta\sigma_{xx}^{\text{MT}(\text{reg2})} = \frac{\pi^2 e^2 \ln \frac{\pi^2}{2\gamma_\phi}}{192 \ln^2 t}. \quad (\text{B14})$$

Despite the presence of the large logarithm $\ln \frac{\pi^2}{2\gamma_\phi}$ in this result in its numerator is relatively small with respect to Eq. (B9) due to the large $\ln^2 t$ in denominator of Eq. (B12).

Fields close to the line $H_{c2}(T)$. — As it was done in the case of the paraconductivity, let us use in Eq. (B7)

domain	$\delta\sigma_{xx}^{\text{MT(an)}} + \delta\sigma_{xx}^{\text{MT(reg2)R}}$	$\delta\sigma_{xx}^{\text{MT(reg1)}}$	$\delta\sigma_{xx}^{\text{MT}}$
I	$\frac{e^2}{8} \frac{1}{\epsilon - \gamma_\phi} \ln \frac{\epsilon}{\gamma_\phi} - \frac{7\zeta(3)e^2}{\pi^4} \ln \left(\frac{1}{\epsilon} \right)$	$-\frac{7\zeta(3)e^2}{\pi^4} \ln \frac{1}{\epsilon}$	$\frac{e^2}{8} \frac{1}{\epsilon - \gamma_\phi} \ln \frac{\epsilon}{\gamma_\phi} - \frac{14\zeta(3)e^2}{\pi^4} \ln \left(\frac{1}{\epsilon} \right)$
I - III	$\frac{e^2}{8} \frac{1}{\epsilon - \gamma_\phi} \left[\psi \left(1/2 + \frac{t\epsilon}{2h} \right) - \psi \left(1/2 + \frac{t\gamma_\phi}{2h} \right) \right] - \frac{7\zeta(3)e^2}{\pi^4} \left[\ln \left(\frac{t}{2h} \right) - \psi \left(1/2 + \frac{t\epsilon}{2h} \right) \right]$	$-\frac{7\zeta(3)e^2}{\pi^4} \left[\psi \left(\frac{t}{2h} \right) - \psi \left(\frac{1}{2} + \frac{t\epsilon}{2h} \right) \right]$	$\frac{e^2}{8} \frac{1}{\epsilon - \gamma_\phi} \left[\psi \left(1/2 + \frac{t\epsilon}{2h} \right) - \psi \left(1/2 + \frac{t\gamma_\phi}{2h} \right) \right] - \frac{14\zeta(3)e^2}{\pi^4} \left[\ln \left(\frac{t}{2h} \right) - \psi \left(1/2 + \frac{t\epsilon}{2h} \right) \right]$
VII	$\frac{e^2}{4} \frac{t}{h - h_{c2}(t)}$	$-\frac{e^2}{4} \frac{t}{h - h_{c2}(t)} - \frac{2e^2}{\pi^2} \ln \frac{2h}{\pi^2 t}$	$-\frac{2e^2}{\pi^2} \ln \frac{2h}{\pi^2 t}$
VI	$\frac{2\gamma_F e^2}{\pi^2} \frac{t}{h}$	$-\frac{2\gamma_F e^2}{\pi^2} \frac{t}{h} - \frac{2e^2}{\pi^2} \ln \frac{2h}{\pi^2 t}$	$-\frac{2e^2}{\pi^2} \ln \frac{2h}{\pi^2 t}$
IV	$\frac{4e^2 \gamma_F^2 t^2}{3\pi^2 h^2}$	$-\frac{2\gamma_F e^2}{\pi^2} \frac{t}{h(t)} - \frac{2e^2}{\pi^2} \left[\ln \frac{1}{2h(t)} \right]$	$-\frac{2e^2}{\pi^2} \left[\ln \frac{1}{2h} \right] - \frac{2\gamma_F e^2}{\pi^4} \frac{t}{h}$
IX	$\frac{7\zeta(3)\pi^2 e^2}{768} \frac{t^2}{h^2} \ln^{-2} \frac{2h}{\pi^2}$	$-\frac{e^2}{\pi^2} \left(\ln \ln \frac{1}{T_{c0}\tau} - \ln \ln \frac{2h}{\pi^2} \right)$	$-\frac{e^2}{\pi^2} \left(\ln \ln \frac{1}{T_{c0}\tau} - \ln \ln \frac{2h}{\pi^2} \right) + \frac{7\zeta(3)\pi^2 e^2}{768} \frac{t^2}{h^2} \ln^{-2} \frac{2h}{\pi^2}$
VIII	$\frac{\pi^2 e^2}{192} \frac{\ln \frac{\pi^2}{2\gamma_\phi}}{\ln^2 t}$	$-\frac{e^2}{\pi^2} \left[\ln \ln \frac{1}{T_{c0}\tau} - \ln \ln t \right]$	$-\frac{e^2}{\pi^2} \left[\ln \ln \frac{1}{T_{c0}\tau} - \ln \ln t \right] + \frac{\pi^2 e^2}{192} \frac{\ln \frac{\pi^2}{2\gamma_\phi}}{\ln^2 t}$

TABLE III. Asymptotic behavior of the MT contributions in different domains, see also Fig. 5 and table II

The analytical continuation of the first one is trivial and it gives the first contribution to the conductivity, which in Landau representation takes the form

$$\delta\sigma_{xx}^{(4,1)} = \left(\frac{2e^2}{\pi^4} \right) \left(\frac{h}{t} \right) \sum_{m=0}^M \sum_{k=0}^{\infty} \frac{\mathcal{E}_m''(t, h, k)}{\mathcal{E}_m(t, h, k)}$$

$$\delta\sigma_{xx}^{(3+4)} = \frac{4e^2}{\pi^4} \left(\frac{h}{t} \right) \sum_{m=0}^M \left[\sum_{k=0}^{\infty} \frac{\mathcal{E}_m''(t, h, k)}{\mathcal{E}_m(t, h, k)} + \frac{\pi}{2} \int_{-\infty}^{\infty} \frac{dx}{\sinh^2(\pi x)} \frac{\text{Im} \mathcal{E}_0(t, h, ix) \text{Im} \mathcal{E}_0'(t, h, ix)}{\text{Re}^2 \mathcal{E}_0(t, h, ix) + \text{Im}^2 \mathcal{E}_0(t, h, ix)} \right]. \quad (\text{C3})$$

Next, we discuss diagram 5. Its contribution can be written in the same way as above:

$$Q_{xx}^{(5)}(\omega_\nu) = \frac{e^2 T^2 v_F^2}{2\pi\nu_0\tau} \int \frac{d^2 q}{(2\pi)^2} \sum_{n,k} L(q, \Omega_k) \lambda^2(q, \epsilon_n, \Omega_{k-n}) \times I^{(5)}(\epsilon_n, \epsilon_{n+\nu}) I^{(5)}(\epsilon_n, -\epsilon_{n-k}),$$

where the integral

$$I^{(5)}(\epsilon_n, \epsilon_{n+\nu}) = \int \frac{d^2 p}{(2\pi)^2} G^2(p, \epsilon_n) G(p, \epsilon_{n+\nu}) = 2\pi i \nu_0 \tau^2 \text{sgn} \epsilon_{n+\nu} \Theta(-\epsilon_{n+\nu} \epsilon_n). \quad (\text{C4})$$

As result:

$$Q_{xx}^{(5)}(\omega_\nu) = -4\pi\nu_0 D e^2 T^2 \int \frac{d^2 q}{(2\pi)^2} \sum_{k=-\infty}^{\infty} L(q, \Omega_k) \times \sum_{n=-\nu}^{-1} \frac{\Theta(\Omega_k - \epsilon_n)}{[2\epsilon_n - \Omega_k + \mathcal{D}\mathbf{q}^2]^2}. \quad (\text{C5})$$

Further evaluation of this expression is very similar to that one of $\tilde{Q}_{xx}^{(5)}(\omega_\nu)$. In particular, after summation over fermionic frequencies, $Q_{xx}^{(7)}(\omega_\nu)$ is presented in the form

The analytical continuation of $\tilde{Q}_{xx}^{(4,2)}(\omega_\nu)$ is completely analogous to that one performed above in the case of the anomalous MT part. As a result the total contribution of diagrams 3 and 4 can be presented as a sum of two very different terms

of two sums over bosonic frequencies, one in the limits $k \in [0, \infty)$, the other $k \in [1, \nu - 1]$ and following step-by-step the same procedure of the analytical continuation as before, one finds that $\delta\sigma_{xx}^{(5,1)} = -\delta\sigma_{xx}^{(4,1)}$, and $\delta\sigma_{xx}^{(5,2)} = \delta\sigma_{xx}^{(4,2)}$. Therefore we get

$$\delta\sigma_{xx}^{(5+6)} = \frac{4e^2}{\pi^4} \left(\frac{h}{t} \right) \sum_{m=0}^M \left[- \sum_{k=0}^{\infty} \frac{\mathcal{E}_m''(t, h, k)}{\mathcal{E}_m(t, h, k)} + \frac{\pi}{2} \int_{-\infty}^{\infty} \frac{dx}{\sinh^2(\pi x)} \frac{\text{Im} \mathcal{E}_0(t, h, ix) \text{Im} \mathcal{E}_0'(t, h, ix)}{\text{Re}^2 \mathcal{E}_0(t, h, ix) + \text{Im}^2 \mathcal{E}_0(t, h, ix)} \right]. \quad (\text{C6})$$

Evaluating the sum and integral close to T_{c0} one can see that the first term in Eq. (C3) is twice larger than the second one. Comparing Eq. (C3) to Eq. (C6) we obtain the old result: $3\delta\sigma_{xx}^{(5+6)} = -\delta\sigma_{xx}^{(3+4)}$, [9], used later in Refs. [1, 5, 6, and 15]. But it is necessary to stress, that the last statement *is not universal*: far from the critical temperature, or at low temperatures, close to $H_{c2}(0)$, the integrals in Eqs. (C3) - (C6) are small with respect to the contribution of the sums. Regarding the latter, they enter in Eqs. (C3) - (C6) with the opposite sign. After the summation in $\delta\sigma_{xx}^{(5-8)}$ these just cancel each other (in this region of temperatures $\delta\sigma_{xx}^{(3+4)} \approx -\delta\sigma_{xx}^{(5+6)}$). To avoid misunderstanding¹⁵, it is more convenient to use the total contribution of the DOS-like diagrams 3-6 in the form:

$$\delta\sigma_{xx}^{\text{DOS}} = \frac{4e^2 h}{\pi^3 t} \sum_{m=0}^M \int_{-\infty}^{\infty} \frac{dx}{\sinh^2 \pi x} \frac{\text{Im } \mathcal{E}_m(t, h, ix) \text{Im } \mathcal{E}'_m(t, h, ix)}{\text{Re}^2 \mathcal{E}_m(t, h, ix) + \text{Im}^2 \mathcal{E}_m(t, h, ix)}. \quad (\text{C7})$$

2. Asymptotic behavior

a. Vicinity of T_{c0} , fields $h \ll 1$ ($H \ll H_{c2}(0)$)

In this case $\ln t = \epsilon \ll 1$, the ψ -function in Eq.(A14) can be expanded. The function $\mathcal{E}_m(t, h, ix)$ is determined by Eq.(A16). Its substitution to Eq.(C7) results in

$$\begin{aligned} \delta\sigma_{xx}^{\text{DOS}} &= -\frac{14\zeta(3)e^2}{\pi^4} \left[\ln(1/2h) - \psi\left(1/2 + \frac{\epsilon}{2h}\right) \right] \\ &= -\frac{14\zeta(3)e^2}{\pi^4} \begin{cases} \ln(1/\epsilon), & h \ll \epsilon \\ \ln\left(\frac{1}{2h}\right), & \epsilon \ll h \ll 1 \end{cases} \quad (\text{C8}) \end{aligned}$$

This expression is valid in the vicinity of the critical temperature T_{c0} and exactly reproduces existing results^{5,6}.

b. High temperatures, high fields

Next, we discuss the high-temperature asymptotic. As it was done above, we assume $\ln t \gg 1$ and use Eqs. (A14)-(A20). The sum over Landau levels in this case converges at large $m_{\text{max}} \sim t/h \gg 1$ and can be substituted by an integral. The main integral contribution comes only from the region up to $x \sim 1$ and can be performed first. One gets

$$\delta\sigma_{xx}^{\text{DOS}} = -\frac{\pi^2 e^2}{192 \ln^2 t}.$$

We see that this result differs from that one of Ref. [9]. The cancellation of the sums of Eqs. (C3) - (C6) in $\delta\sigma_{xx}^{\text{DOS}}$ removes the double logarithmic term $\ln \ln t$ from it. Nevertheless, such terms in $\delta\sigma_{xx}^{(\text{tot})}$ still appear from the regular MT term and, as we will see below, from diagrams 9 and 10.

In the limit of high fields $h \gg t$ the summation over Landau levels gives:

$$\delta\sigma_{xx}^{\text{DOS}} = -\frac{7\zeta(3)\pi^2 e^2}{384} \left(\frac{t}{h}\right)^2 \frac{1}{\ln^2 \frac{2h}{\pi^2}}.$$

c. Above the line $H_{c2}(T)$ but $t \ll h_{c2}(t)$

Using the asymptotic Eq. (A22) one can perform the integration in Eq. (C7) and express $\delta\sigma_{xx}^{\text{DOS}}$ in terms of the integral J_{GL} :

$$\delta\sigma_{xx}^{\text{DOS}} = -\frac{e^2}{\pi^2} \sum_{m=0}^M \frac{J_{GL} \left[\frac{4h(2m+1)}{\pi^2 t} \ln \frac{4h}{\pi^2} \left(m + \frac{1}{2}\right) \right]}{(2m+1)}.$$

Close to the line $H_{c2}(T)$ we can restrict ourselves to the LLL and immediately get

$$\delta\sigma_{xx}^{\text{DOS}} = -\frac{e^2}{\pi^2} J_{GL} \left(\frac{4\tilde{h}}{\pi^2 t} \right).$$

Looking on the asymptotic behavior of $J(r)$ at low temperatures, one notices that in contrast to the statement of Ref [15] the group of diagrams 5-8 does not give any contribution to $\delta\sigma_{xx}^{(\text{tot})}$ when temperature tends to zero. Nevertheless, a non-trivial contribution of quantum fluctuations $\sim \ln \tilde{h}$, found in Ref. [15], exists due to the regular MT term and diagrams 9 and 10.

Appendix D: Renormalization of the diffusion coefficient: contribution of diagrams 7-10

1. General expression

We start with the calculation of diagram 7:

$$\begin{aligned} Q_{xx}^{(7)}(\omega_\nu) &= 2e^2 T^2 \sum_{k,n} \int \frac{d^2 q}{(2\pi)^2} L(q, \Omega_k) \lambda(\mathbf{q}, \varepsilon_n, \Omega_k - \varepsilon_n) \\ &\lambda(\mathbf{q}, \varepsilon_{n+\nu}, \Omega_k - \varepsilon_{n+\nu}) C(q, \varepsilon_{n+\nu}, \Omega_k - \varepsilon_n) I_1^{(7)} I_2^{(7)}, \quad (\text{D1}) \end{aligned}$$

where the integrals of the Green's function products can be calculated in the standard way:

$$\begin{aligned} I_{(1)}^{(7)}(\varepsilon_n, \varepsilon_{n+\nu}, \Omega_{k-n}) &= \int \frac{d^D p}{(2\pi)^D} v_x(p) G(p, \varepsilon_n) G(p, \varepsilon_{n+\nu}) \\ &\times G(q-p, \Omega_{k-n}) = 4\pi\nu_0 \mathcal{D}\mathbf{q} x \tau^2 \theta(\varepsilon_n \varepsilon_{n+\nu}) \theta(-\varepsilon_n \Omega_{k-n}) \quad (\text{D2}) \end{aligned}$$

$$I_{(2)}^{(7)} = I_{(1)}^{(7)}(\Omega_{k-n-\nu}, \Omega_{k-n}, \varepsilon_{n+\nu}).$$

Substitution of these expressions to Eq. (D1) and accounting for the fact that $\overline{\mathcal{D}\mathbf{q}_x^2} = \mathcal{D}\mathbf{q}^2/2$ results in

$$Q_{xx}^{(7)} = 8\pi\nu_0 \mathcal{D}e^2 T^2 \int \frac{\mathcal{D}\mathbf{q}^2 d^2q}{(2\pi)^2} \sum_{k=-\infty}^{\infty} L(q, \Omega_k) \sum_{n=-\infty}^{\infty} \frac{\theta(-\varepsilon_n(\Omega_k - \varepsilon_n)) \theta(-\varepsilon_{n+\nu}(\Omega_k - \varepsilon_{n+\nu}))}{|2\varepsilon_n - \Omega_k| + \mathcal{D}\mathbf{q}^2} \frac{\theta(\varepsilon_n \varepsilon_{n+\nu})}{|2\varepsilon_{n+\nu} - \Omega_k| + \mathcal{D}\mathbf{q}^2} \frac{\theta(\varepsilon_n \varepsilon_{n+\nu})}{|2\varepsilon_n + \omega_\nu - \Omega_k| + \mathcal{D}\mathbf{q}^2}.$$

The θ -function $\theta(\varepsilon_n \varepsilon_{n+\nu})$ defines the limits of summation over fermionic frequencies n as $(-\infty, -\nu - 1]$ and $[0, \infty)$. Changing the sign of summation in the first interval and then shifting the variable of summation $\varepsilon_n + \omega_\nu \rightarrow \varepsilon_{n'}$, one finds that the expression is even in Ω_k , which allows to present $Q_{xx}^{(7)}(\omega_\nu)$ in the form of an analytical function of ω_ν , to perform the analytical continuation $\omega_\nu \rightarrow -i\omega$, and to expand it over small ω :

$$Q_{xx}^{(7)R}(\omega) = -8\pi\nu_0 \mathcal{D}e^2 T^2 \sum_{k=-\infty}^{\infty} \int \mathcal{D}\mathbf{q}^2 L(q, \Omega_k) \frac{d^2q}{(2\pi)^2} \sum_{n=0}^{\infty} \left\{ \frac{1}{[2\varepsilon_n + |\Omega_k| + \mathcal{D}\mathbf{q}^2]^3} + \frac{3i\omega}{[2\varepsilon_n + |\Omega_k| + \mathcal{D}\mathbf{q}^2]^4} \right\}. \quad (\text{D3})$$

The corresponding contribution to the conductivity is determined by the imaginary part of Eq. (D3). Quantizing the motion of Cooper pairs and going over to the Landau representation, one finds

$$\delta\sigma_{xx}^{(7+8)} = \frac{2e^2}{\pi^6} \left(\frac{\hbar}{t}\right)^2 \sum_{m=0}^M \left(m + \frac{1}{2}\right) \sum_{k=-\infty}^{\infty} \frac{8\mathcal{E}_m'''(t, \hbar, |k|)}{\mathcal{E}_m(t, \hbar, |k|)}. \quad (\text{D4})$$

Comparing this formula with Eq. (B7) one can see that beyond the vicinity of T_{c0} the contribution of diagrams 7 and 8 given by the Eq.(D4) cancels the regular MT contribution [given by the first term of Eq. (B7)].

Finally we proceed with the calculation of diagram 9. Two integrals of the three Green function blocks in it are equal and coincide with $I_1^{(7)}$. Substituting Eq. (D2) to the general expression for $Q_{xx}^{(9)}(\omega_\nu)$ and performing the summation over fermionic frequencies in the spirit of the above calculations, one finds

$$Q_{xx}^{(9)}(\omega_\nu) = -\frac{e^2 T}{4\pi^2 \nu_0 \tau^4 \omega_\nu^2} \sum_{k=-\infty}^{\infty} \int \frac{d^2q}{(2\pi)^2} \mathcal{D}\mathbf{q}^2 L(q, \Omega_k) \times [\Psi_1(|\Omega_k|, \omega_\nu) - \Psi_2(|\Omega_{k+\nu}|, \omega_\nu)] = Q_{(1)}^{(9)} + Q_{(2)}^{(9)}, \quad (\text{D5})$$

where

$$\Psi_\gamma(x, \omega_\nu) = \left[\psi\left(\frac{1}{2} + \frac{\omega_\nu + x + \mathcal{D}\mathbf{q}^2}{4\pi T}\right) - \psi\left(\frac{1}{2} + \frac{x + \mathcal{D}\mathbf{q}^2}{4\pi T}\right) - \frac{\omega_\nu}{(4\pi T)} \psi'\left(\frac{1}{2} + \frac{\omega_\nu}{4\pi T} \delta_{\gamma 2} + \frac{x + \mathcal{D}\mathbf{q}^2}{4\pi T}\right) \right] \quad (\text{D6})$$

with $\gamma = 1, 2$.

There is no problem to perform analytical continuation of the first term of Eq. (D5): the function $\Psi_1(|\Omega_k|, \omega_\nu)$ is analytical in its argument ω_ν , and the corresponding contribution to Eq. (D5) can be continued in the standard way $\omega_\nu \rightarrow -i\omega \rightarrow 0$. Expanding Eq. (D6) with $\gamma = 1$ over ω one finds the essential contribution to the

electromagnetic response operator:

$$Q_{(1)}^{(9)R}(\omega) = -i\omega \frac{\mathcal{D}\nu_0 e^2 T}{3(4\pi T)^3} \sum_{k=-\infty}^{\infty} \int \mathcal{D}\mathbf{q}^2 \frac{d^2q}{(2\pi)^2} \times L(q, \Omega_k) \psi''' \left(\frac{1}{2} + \frac{|\Omega_k| + \mathcal{D}\mathbf{q}^2}{4\pi T} \right). \quad (\text{D7})$$

The evaluation of the second term of Eq. (D5) turns out to be much more sophisticated, since ω_ν appears in $\Psi_2(|\Omega_{k+\nu}|, \omega_\nu)$ not only as parameter but also in the argument $|\Omega_{k+\nu}|$ of this non-analytical function. The situation is analogous to the AL contribution and the same method of analytical continuation has to be applied. The corresponding sum over bosonic frequencies is transformed in an integral over the contour \mathcal{C} shown in Fig. 11 with three regions of different analytic behavior:

$$Q_{(2)}^{(9)}(\omega_\nu) = \frac{1}{2\pi i} \frac{\mathcal{D}\nu_0 e^2}{\omega_\nu^2} \int \mathcal{D}\mathbf{q}^2 \frac{d^2q}{(2\pi)^2} \times \oint_{\mathcal{C}} \coth \frac{z}{2T} L(q, -iz) \psi_1(|\Omega_{k+\nu}|, \omega_\nu).$$

After shifting of the variable z of the integral over the line $\text{Im}z = -\omega_\nu$ as $-iz + \omega_\nu \rightarrow -iz'$, one gets $Q_{(2)}^{(9)}(\omega_\nu)$ already as an analytical function of ω_ν :

$$Q_{(2)}^{(9)}(\omega_\nu) = \frac{\mathcal{D}\nu_0 e^2}{\pi \omega_\nu^2} \int \mathcal{D}\mathbf{q}^2 \frac{d^2q}{(2\pi)^2} \int_{-\infty}^{\infty} dz \coth\left(\frac{z}{2T}\right) \times [\Psi_2^R(-iz + \omega_\nu, \omega_\nu) \text{Im}L^R(q, -iz) + L^A(q, -iz - \omega_\nu) \text{Im}\Psi_2^R(-iz, \omega_\nu)]. \quad (\text{D8})$$

Obviously, this expression can be continued in ω_ν in the standard way $\omega_\nu \rightarrow -i\omega$.

We are interested in the imaginary part of $Q_{(2)}^{(9)R}(\omega)$, i.e. only $\text{Im}\Psi_2^R(-iz - i\omega, -i\omega)$ and $\text{Im}\Psi_2^R(-iz, -i\omega)$ are essential. They can be written explicitly from Eq. (D6):

$$\text{Im}\Psi_2^R(-iz, -i\omega) = -\frac{\omega^3}{3(4\pi T)^4} \text{Re}\psi''' \left(\frac{1}{2} + \frac{-iz + \mathcal{D}\mathbf{q}^2}{4\pi T} \right) \quad (\text{D9})$$

with $\text{Im}\Psi_2^R(-iz - i\omega, -i\omega) = 5\text{Im}\Psi_2^R(-iz, -i\omega)$. Since we are interested only in the linear ω -part of $\text{Im}Q_{(2)}^{(9)R}(\omega)$ in the analytically continued Eq. (D8), one can omit $i\omega$ in the argument of $L^A(q, -iz + i\omega)$ and recall that $\text{Im}L^A(q, -iz) = -\text{Im}L^R(q, -iz)$. One gets:

$$\text{Im}Q_{(2)}^{(9)}(\omega) = \frac{4\omega D\nu_0 e^2}{3\pi(4\pi T)^4} \int \mathcal{D}\mathbf{q}^2 \frac{d^2q}{(2\pi)^2} \int_{-\infty}^{\infty} dz \coth\left(\frac{z}{2T}\right) \times \text{Re}\psi''' \left(\frac{1}{2} + \frac{-iz + \mathcal{D}\mathbf{q}^2}{4\pi T} \right) \text{Im}L^R(q, -iz).$$

Now one can see that the integrand function is odd in z and its integration with symmetric limits gives zero. Hence, in linear approximation $\text{Im}Q_{(2)}^{(9)}(\omega) = 0$ and the second term of Eq. (D5) does not contribute to conductivity. Going over to the dimensionless variables in Eq. (D7) and to the Landau representation, one finds that $\delta\sigma_{xx}^{(9)} = -\delta\sigma_{xx}^{(7)}/3$. Finally, the total contribution of diagrams 7-10, determining the renormalization of the one-particle diffusion coefficient in the presence of superconducting fluctuations, is

$$\delta\sigma_{xx}^{7-10} = \frac{4e^2}{3\pi^6} \left(\frac{h}{t}\right)^2 \sum_{m=0}^M \sum_{k=-\infty}^{\infty} \left(m + \frac{1}{2}\right) \frac{8\mathcal{E}_m'''(t, h, |k|)}{\mathcal{E}_m(t, h, |k|)}. \quad (\text{D10})$$

2. Asymptotic behavior

a. Vicinity of T_{c0} , fields $h \ll 1$ ($H \ll H_{c2}(0)$)

In contrast to the AL, MT and DOS contributions, due to presence of the multiplier $\mathcal{D}\mathbf{q}^2$ in the numerator of Eq. (D5) [corresponding to $(m + \frac{1}{2})$ in Eq. (D10) close to the critical temperature T_{c0}], the value $\delta\sigma_{(2)}^{(DCR)}$ turns out to be not singular in ϵ at all. Substituting the summations in Eq. (D10) by integrals, one finds

$$\delta\sigma_{xx}^{7-10}(\epsilon \ll 1) = \frac{e^2}{3\pi^2} \ln \ln \frac{1}{T_{c0}\tau} + O(\epsilon), \quad (\text{D11})$$

which just gives a temperature independent constant. Let us stress that this constant is necessary for matching of the results in domain I and VII of Fig. 5.

b. High temperatures, high fields

In this domain of the phase diagram, we cannot omit $\ln t \gg 1$ in the denominator of Eq. (D10), but the above consideration still is applicable. As a result we get

$$\delta\sigma_{xx}^{7-10}(t \gg \max\{1, h\}) = \frac{e^2}{3\pi^2} \left(\ln \ln \frac{1}{T_{c0}\tau} - \ln \ln t \right). \quad (\text{D12})$$

In the limit of high fields $h \gg t$

$$\delta\sigma_{xx}^{7-10}(h \gg \max\{1, t\}) = \frac{e^2}{3\pi^2} \left(\ln \ln \frac{1}{T_{c0}\tau} - \ln \ln \frac{2h}{\pi^2} \right). \quad (\text{D13})$$

c. Above the line $H_{c2}(T)$ but $t \ll h_{c2}(t)$

In this region one can restrict the consideration to the LLL approximation and use the asymptotic expression (A22). In complete analogy with the case of the regular part of the MT contribution one finds

$$\delta\sigma_{xx}^{7-10}(t \ll 1, \tilde{h}) = \frac{4e^2}{3\pi^2} \ln \frac{1}{\tilde{h}}. \quad (\text{D14})$$

One can notice the close connection between the $\delta\sigma_{xx}^{7-10}$ and the $\delta\sigma_{xx}^{\text{MT}(\text{reg1})}$ contributions, which is why the Eqs. (D11)-(D14) should be considered side by side with Eqs. (B8)-(B12).

¹ A.I. Larkin, A.A. Varlamov, *Theory of Fluctuations in Superconductors*, OUP, Second Edition, (2009).

² L.G. Aslamazov, and A.I. Larkin, *Soviet Solid State Physics*, **10**, 875 (1968).

³ K. Maki. *Progress in Theoretical Physics*, **39**, 897; *ibid.* **40**, 193 (1968).

⁴ R.S. Thompson, *Physical Review* **B1**, 327 (1970).

⁵ L.B. Ioffe, A.I. Larkin, A.A. Varlamov, Yu. Lu, *Phys. Rev.* **B47**, 8936 (1993);

⁶ V.V. Dorin, R.A. Klemm, A.A. Varlamov, A.I. Buzdin, D.V. Livanov, *Phys. Rev.* **B48**, 12591 (1993).

⁷ L.G. Aslamazov, and A.A. Varlamov, *Journal of Low Temp. Phys.*, **38**, 223 (1980).

⁸ A.I. Larkin, *JETP Letters*, **31**, 219 (1980).

⁹ B.L. Altshuler, M.Yu. Rezyer, A.A. Varlamov, *Soviet JETP*, **57**, 1329 (1983).

¹⁰ J.M.B. Lopes dos Santos, E. Abrahams, *Physical Review*, **B31**, 172 (1985).

¹¹ I.S. Beloborodov, K.B. Efetov, *Phys. Rev. Lett.*, **B82**, 3332 (1999).

¹² I.S. Beloborodov, K.B. Efetov, and A.I. Larkin, *Physical Review*, **B61**, 9145 (2000).

- ¹³ M.A. Skvortsov, M. Serbin, A.A. Varlamov, V. Galitski, *Phys. Rev. Lett.*, **102**, 067001, (2009).
- ¹⁴ It is worth mentioning that the contribution of diagrams 7-10, which represents the renormalization of the diffusion coefficient due to the presence of fluctuations (we will call this group the *DCR* diagrams) was never distinguished from the DOS contributions before. It was believed that these diagrams are not singular at all close to the critical temperature, but far from the critical temperature these form together with diagrams 3-6 long, double logarithmic tails in temperature in the fluctuation conductivity.
- ¹⁵ V. M. Galitski and A. I. Larkin, *Phys. Rev. B* **63**, 174506 (2001); *Phys. Rev. Lett.* **87**, 087001 (2001).
- ¹⁶ Numerical evaluation software and "fluctuoscapy" tools, available at: <http://mti.msd.anl.gov/highlights/FC>
- ¹⁷ K. Jin *et al.*, *Phys. Rev. B* **77**, 172503 (2008); B. Leridon, J. Vanacken, T. Wambecq, and V. Moshchalkov, *Phys. Rev. B* **76**, 012503 (2007); S. Caprara, M. Grilli, B. Leridon, and J. Vanacken, *Phys. Rev. B* **79**, 024506 (2009).
- ¹⁸ V.F. Gantmakher *et al.*, *JETP Letters*, **77**, 498 (2003).
- ¹⁹ L. Reggiani, R. Vaglio, A.A. Varlamov, *Physical Review*, **44**, 9541 (1991).
- ²⁰ M. Steiner, A. Kapitulnik, *Physica C* **422**, 16 (2005).
- ²¹ A.A. Abrikosov *Fundamentals of Metal Theory*, Elsevir, (1988).
- ²² I. V. Lerner, A. A. Varlamov, V. M. Vinokur, *Phys. Rev. Lett.*, **100**, 117003, (2008).
- ²³ Data is courtesy of M. Kartsovnik..